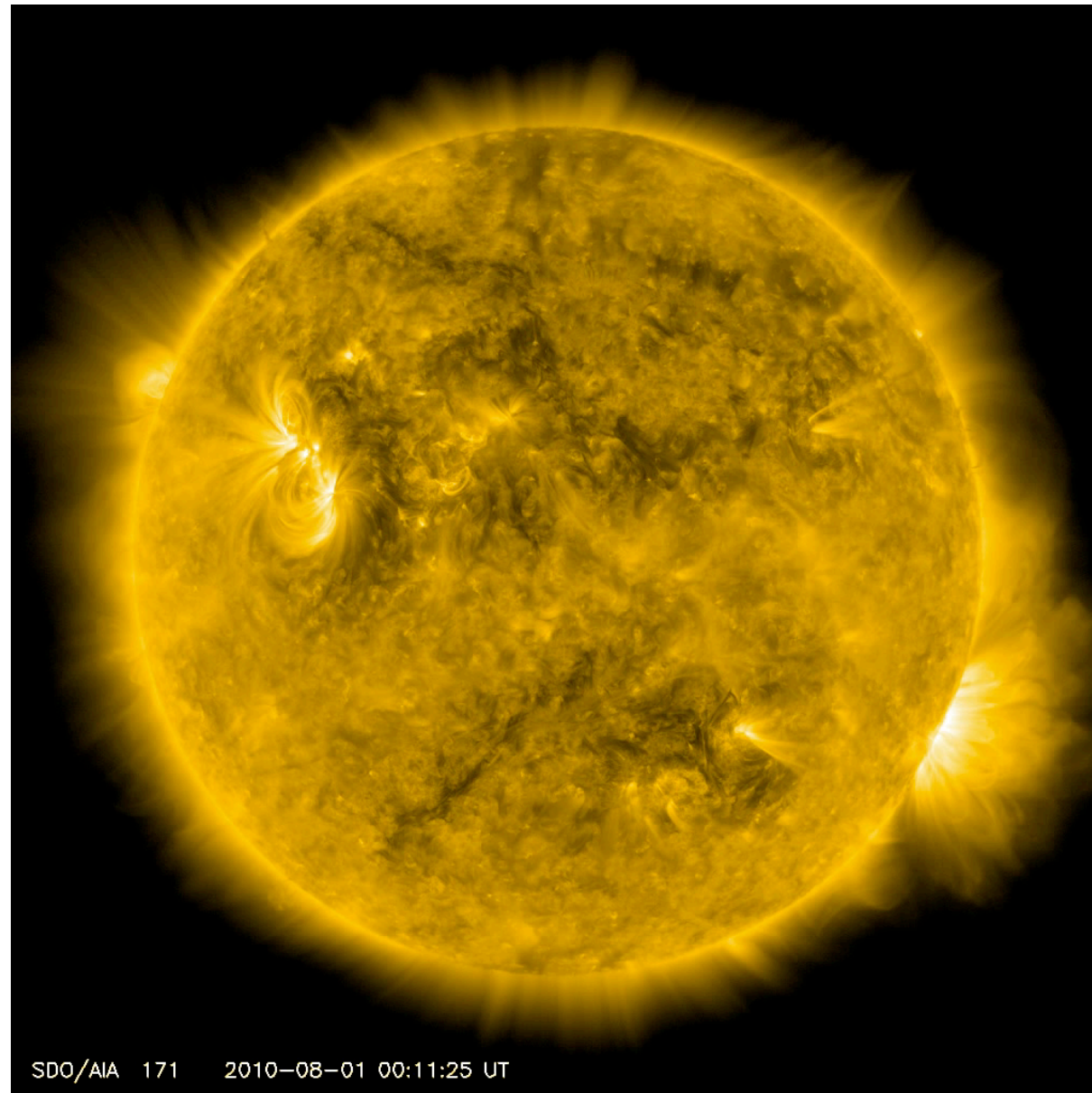


Lecture 5

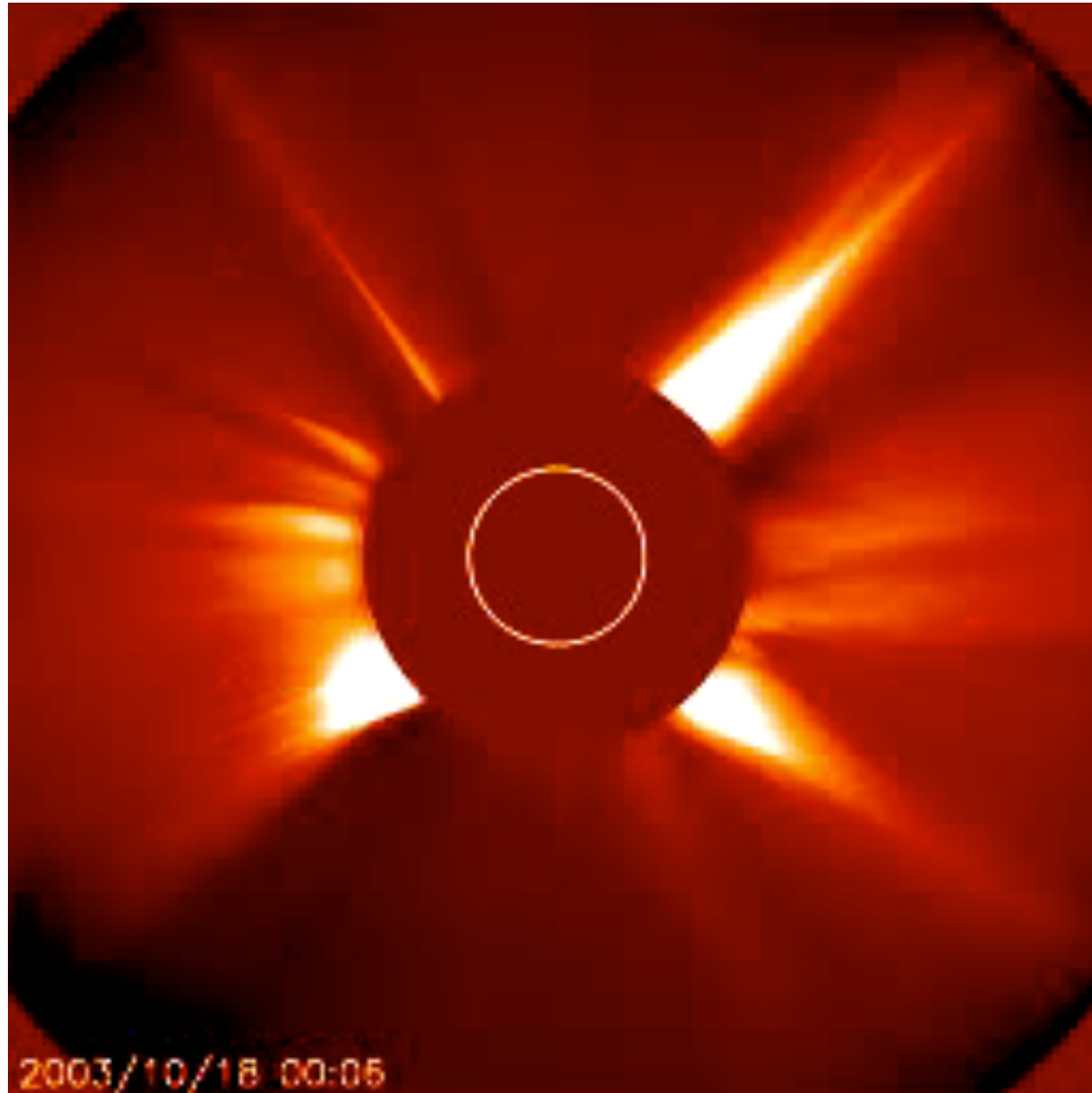
CME Flux Ropes

February 1, 2017

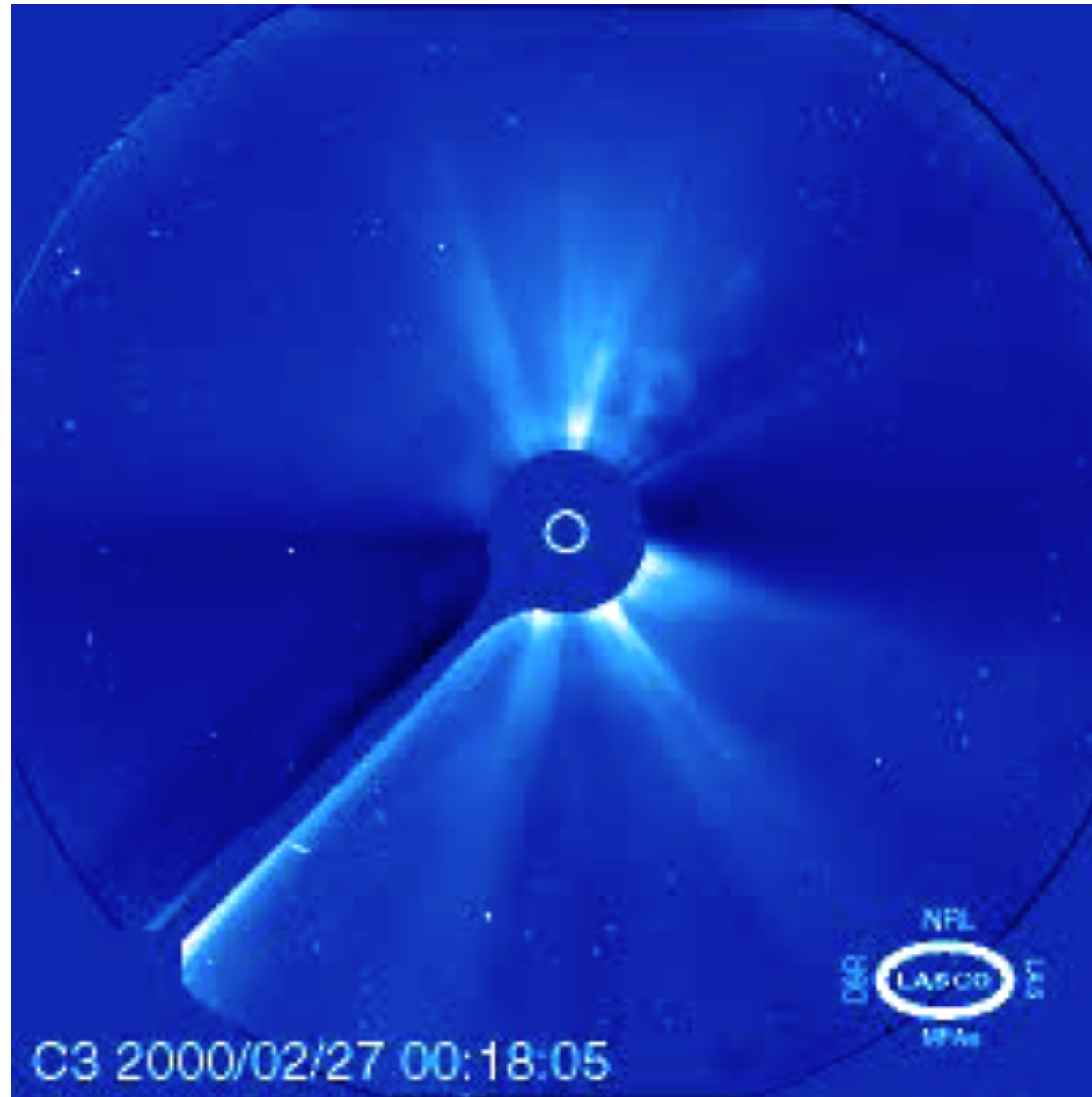
energy release on the Sun in a day



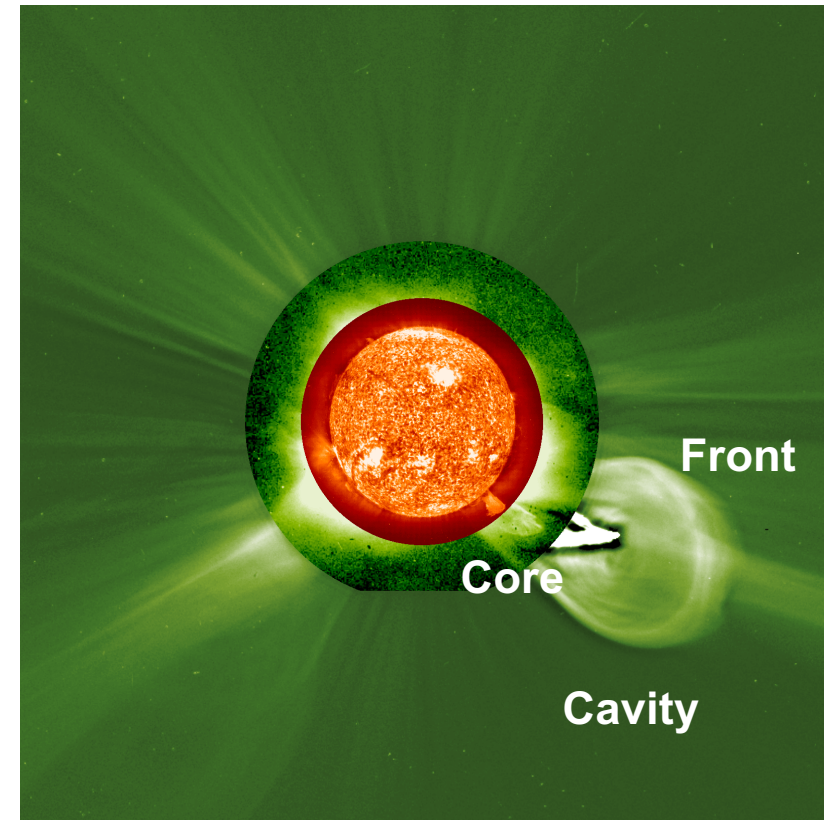
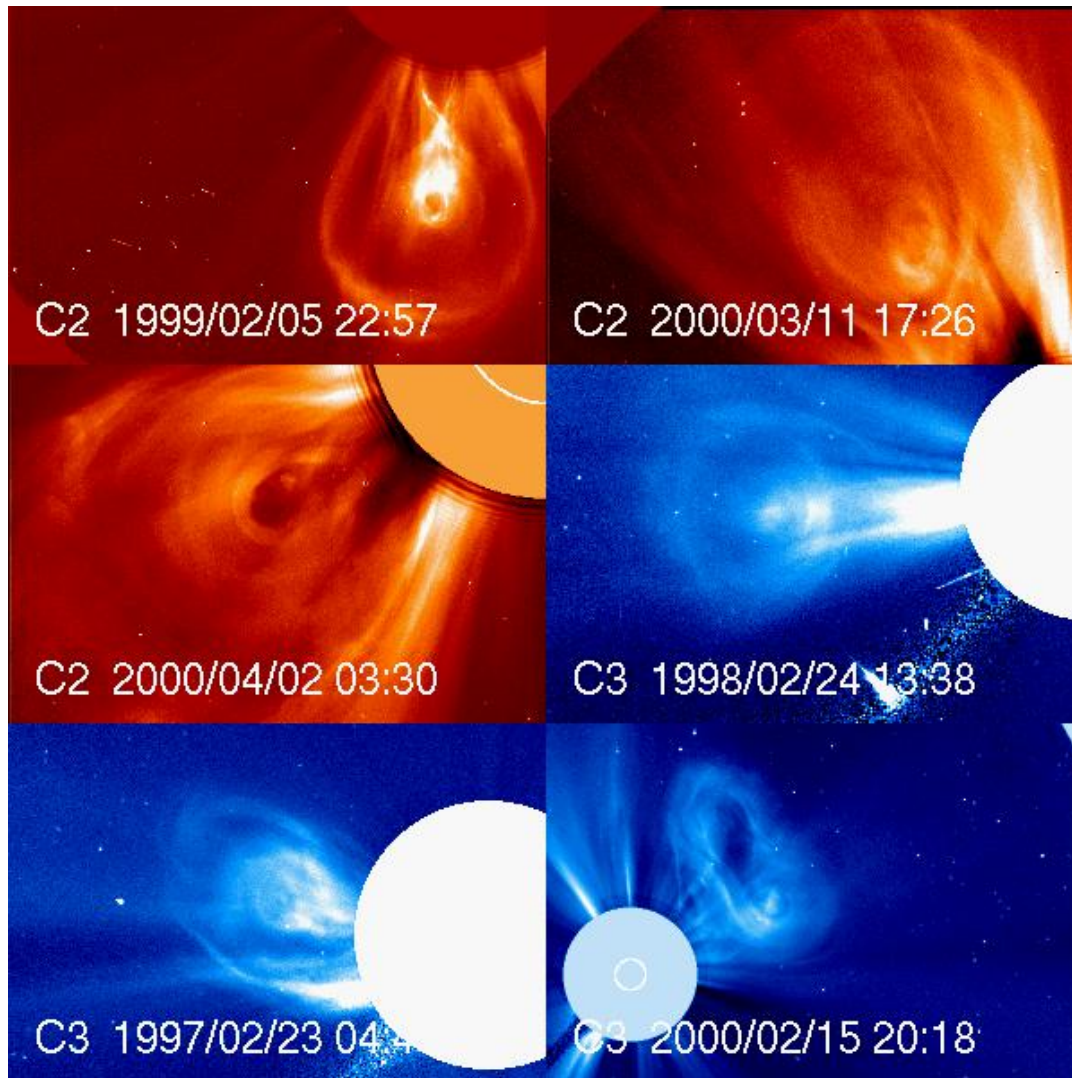
CMEs best seen by coronagraphs – LASCO C2



CMEs best seen by coronagraphs – LASCO C3

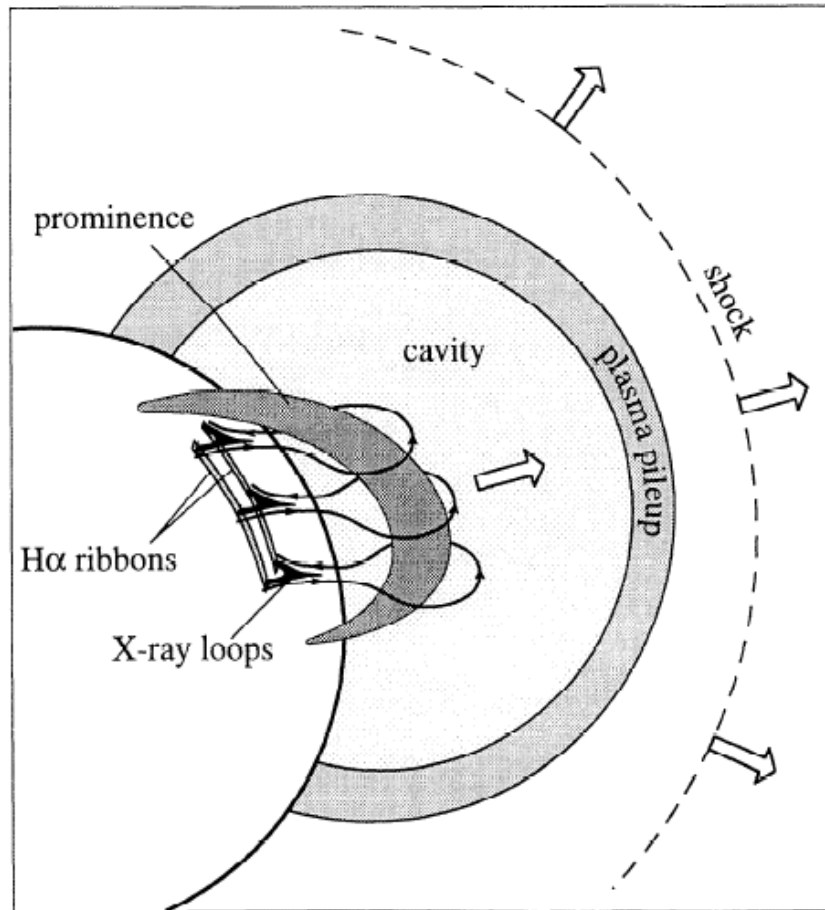


The three-part white light CME

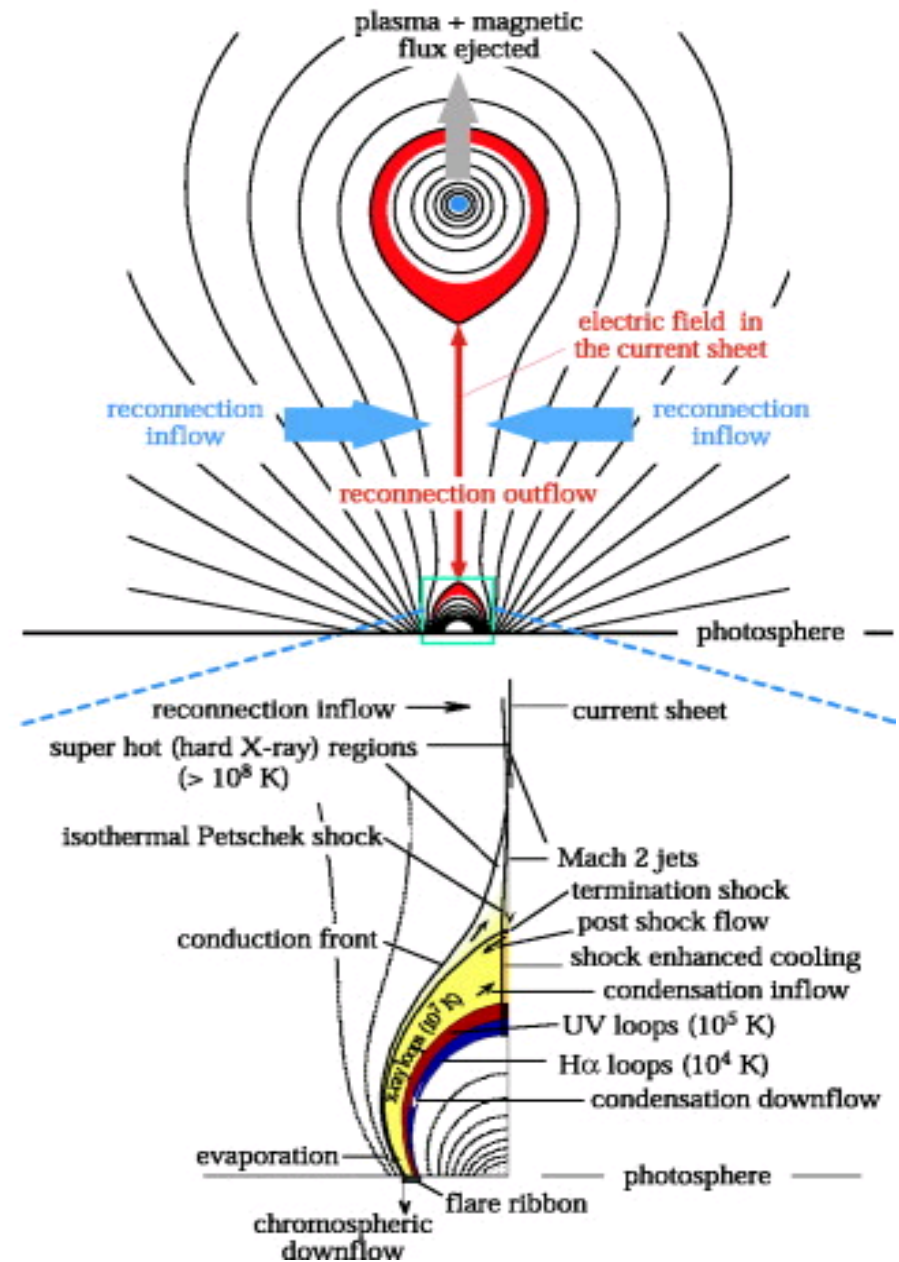


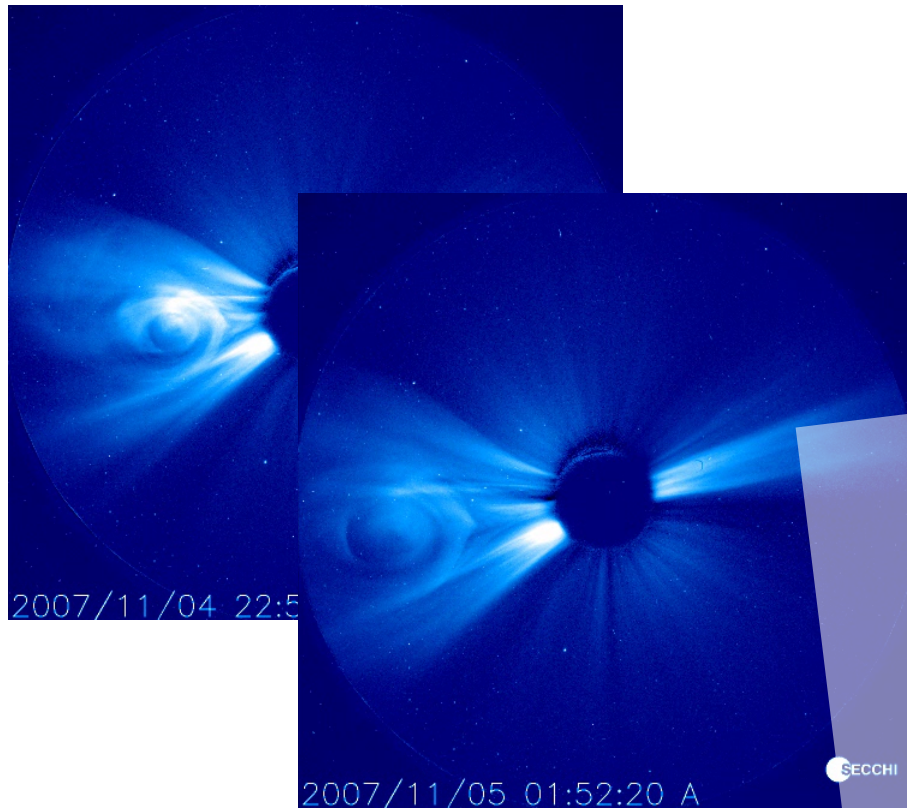
Vourlidas et al 2013

standard flare-CME model

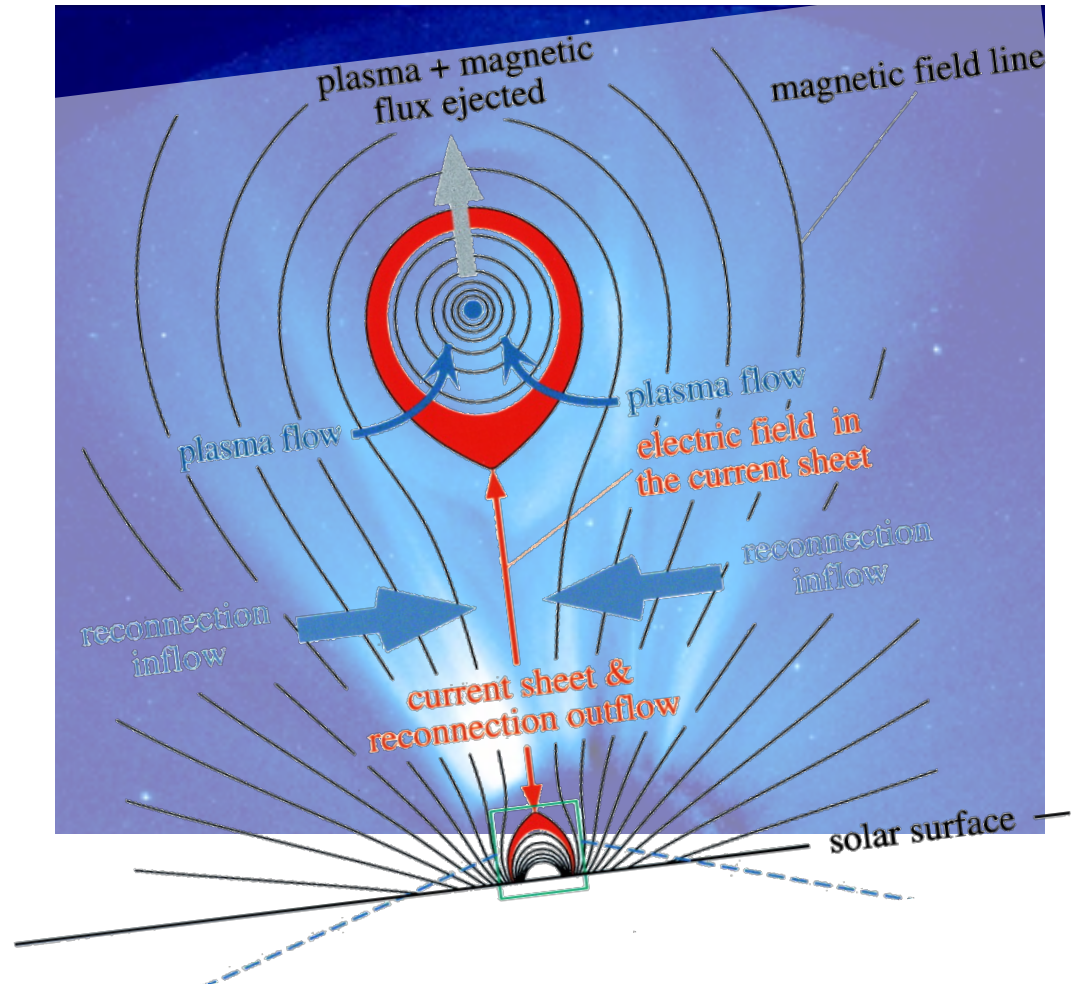


Forbes-Lin model





1. structure
2. genesis
3. energetics



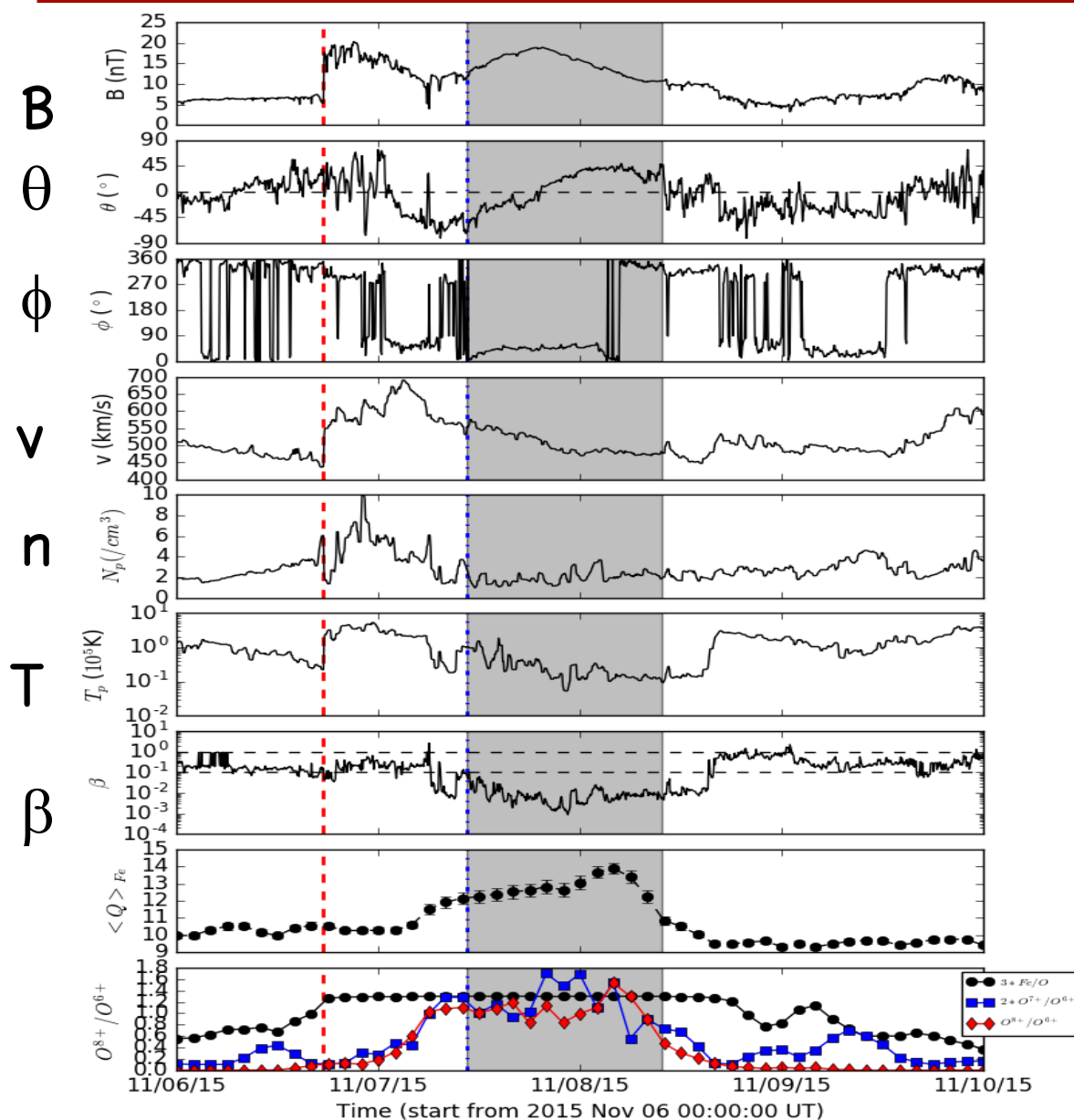
Angelos Vourlidas

Brief History of Magnetic Cloud

- 1954 Morrison: unusual magnetized clouds of plasma emitted by the active sun.
- 1958 Cocconi et al.: magnetic loop or bottle anchored in the sun.
- 1958 Piddington: magnetic bubble detached from the sun by reconnection.
- 1959 Gold: shocks preceding these magnetic loops
- 1980–81 Burlaga: first coined “magnetic cloud”
- 1990, 1997, Lepping: magnetic cloud properties

(Burlaga et al, 1981, JGR, 86, 6673–6684)

In-situ measurements of Magnetic Cloud



Tightly wound helix

B: 10 - 100 nT

Low temperature
 $T: 10^5 \text{ K}$, $n: 10 - 100 \text{ cm}^{-3}$, $\beta: 0.01 - 0.1$

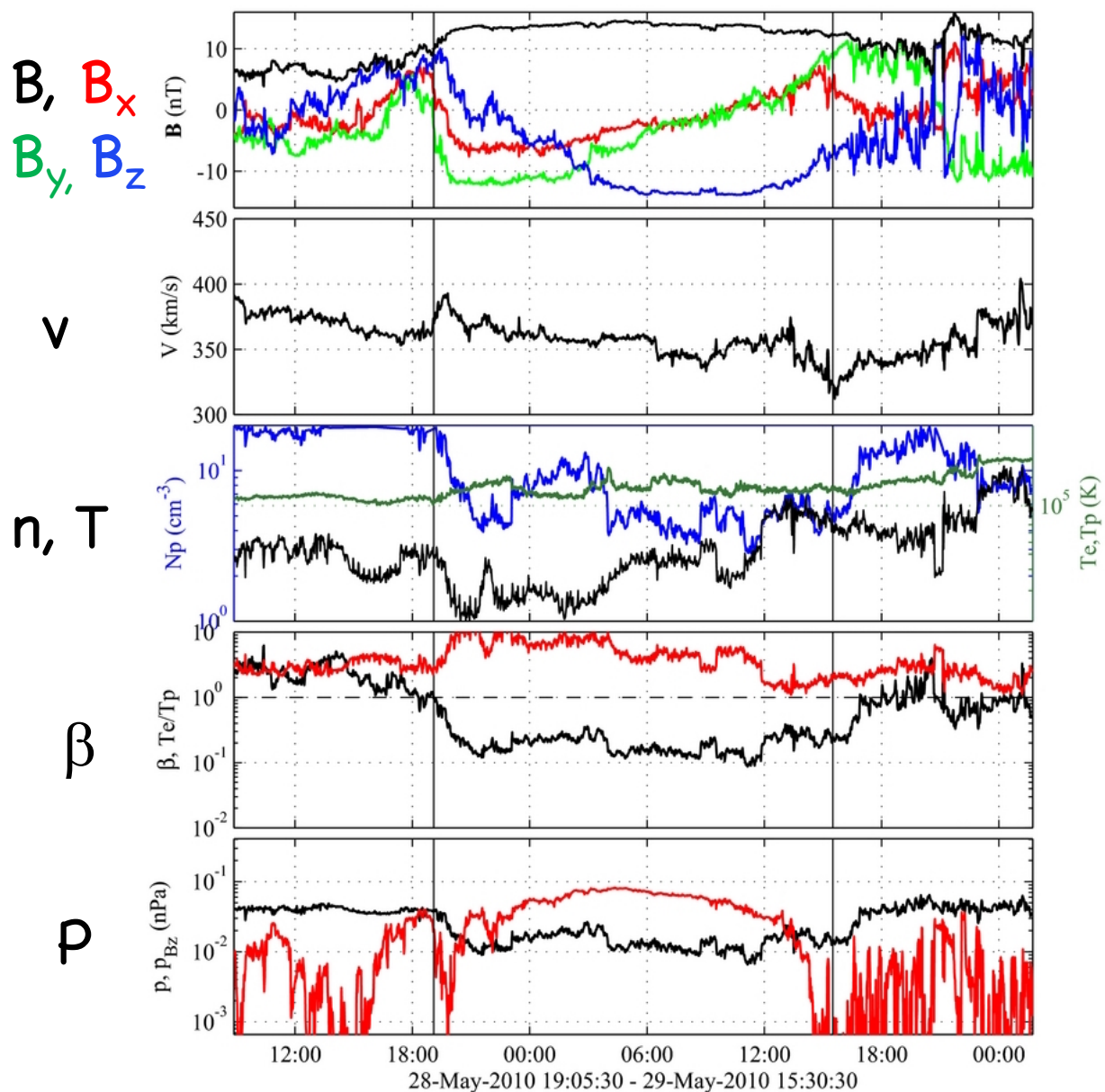
Higher speed than
 ambient solar wind
 $v: 300 - 800 \text{ km s}^{-1}$

Preceded by shocks
 and sheaths

(Burlaga et al 1981;
 Lepping et al. 1990)

Liu R. et al. 2017

In-situ measurements of Magnetic Cloud



Hu et al. 2014

Tightly wound helix
 B : 10 – 100 nT

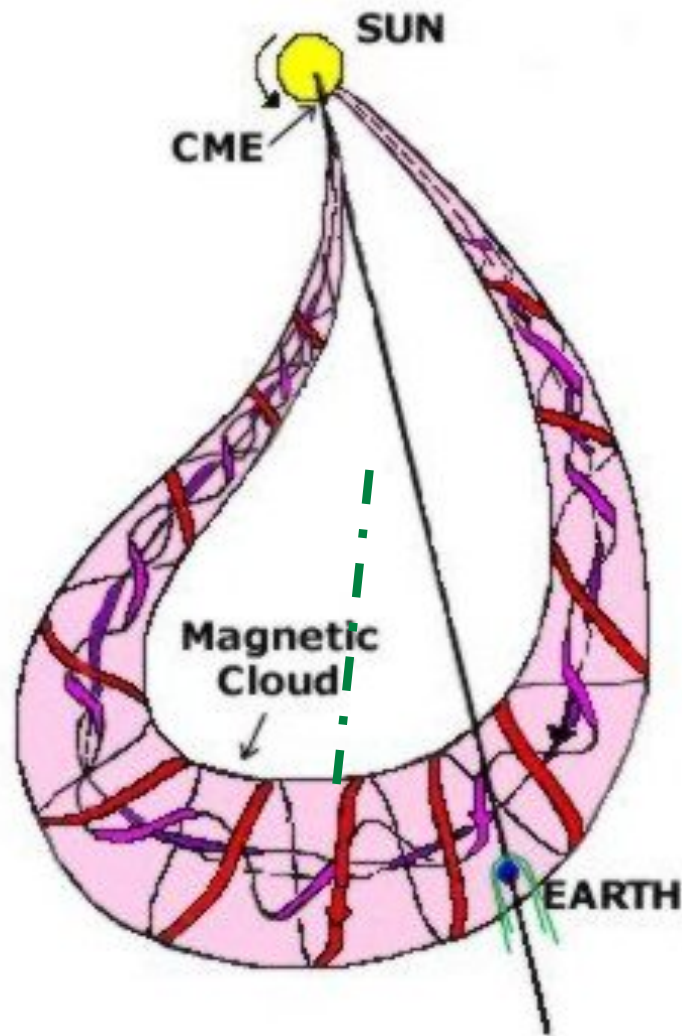
Low temperature
 T : 10^5 K, n : 10 – 100 cm^{-3} , β : 0.01 – 0.1

Higher speed than
 ambient solar wind
 v : 300 – 800 km s^{-1}

Preceded by shocks
 and sheaths

(Burlaga et al 1981;
 Lepping et al. 1990)

Magnetic Cloud: interplanetary flux rope



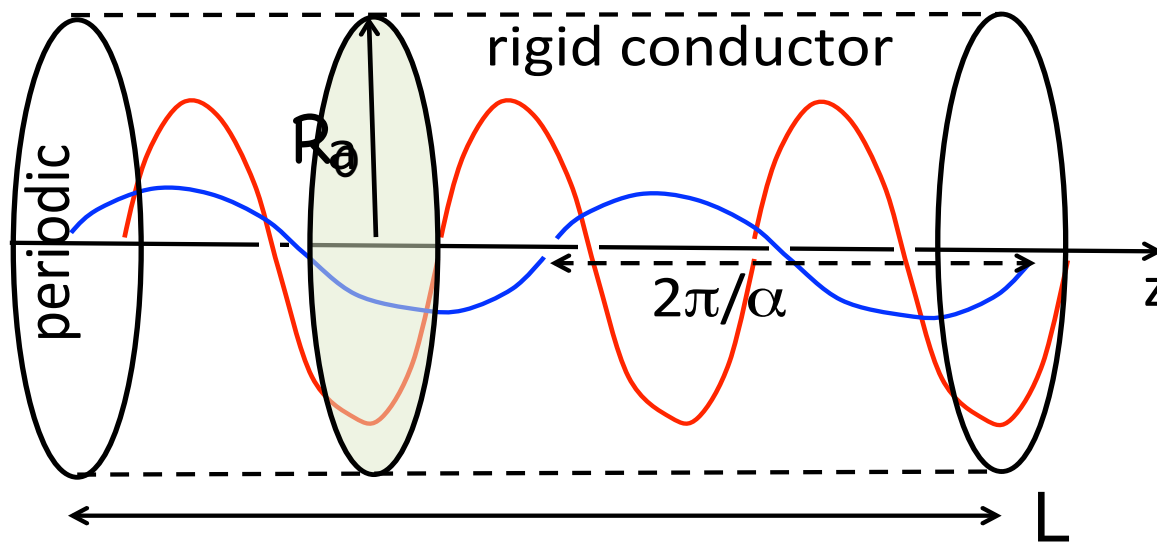
From in-situ observations, a flux rope may be reconstructed with various methods (Riley et al. 2004, Dasso et al. 2006 for a summary of these methods), assuming a 2d cylindrical structure of the CME flux rope.

[After Marubashi]

Not to Scale

MC flux rope: the Lundquist solution

$$\mathbf{B}_0(r) = B_0 \left[J_0(\alpha r) \hat{\mathbf{z}} + J_1(\alpha r) \hat{\phi} \right]$$



Least-squares fitting of the data points to determine 7 parameters, including the rope axis orientation, radius, and axial field B_0 .

(Lepping et al. 1990, Lynch et al. 2005)

toroidal flux:

$$\Phi_t = \iint B_z r dr d\phi$$

poloidal flux:

$$\Phi_p = \iint B_\phi dr dl$$

magnetic helicity:

$$H_m = \int \vec{A} \cdot \vec{B} d^3x$$

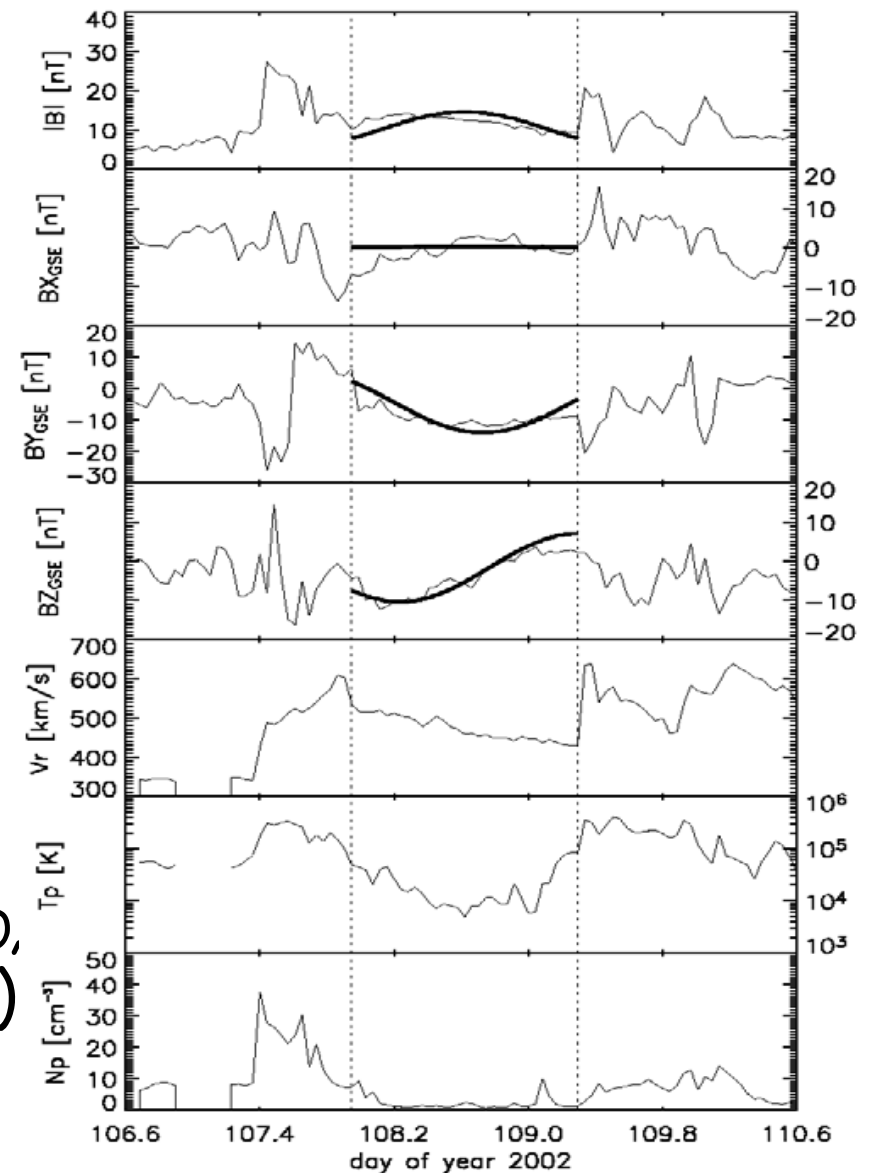
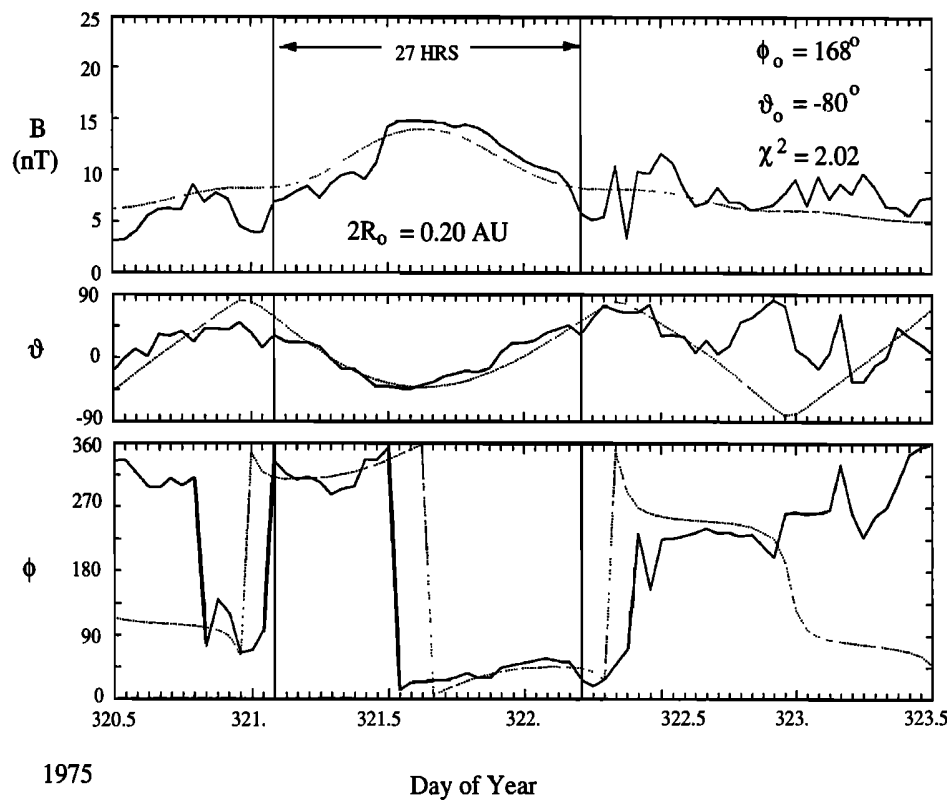
$$= \frac{1}{\alpha} \int B^2 d^3x$$

magnetic twist:

$$T = \frac{l B_\phi}{r B_z}, \quad \tau = \frac{T}{2\pi}$$

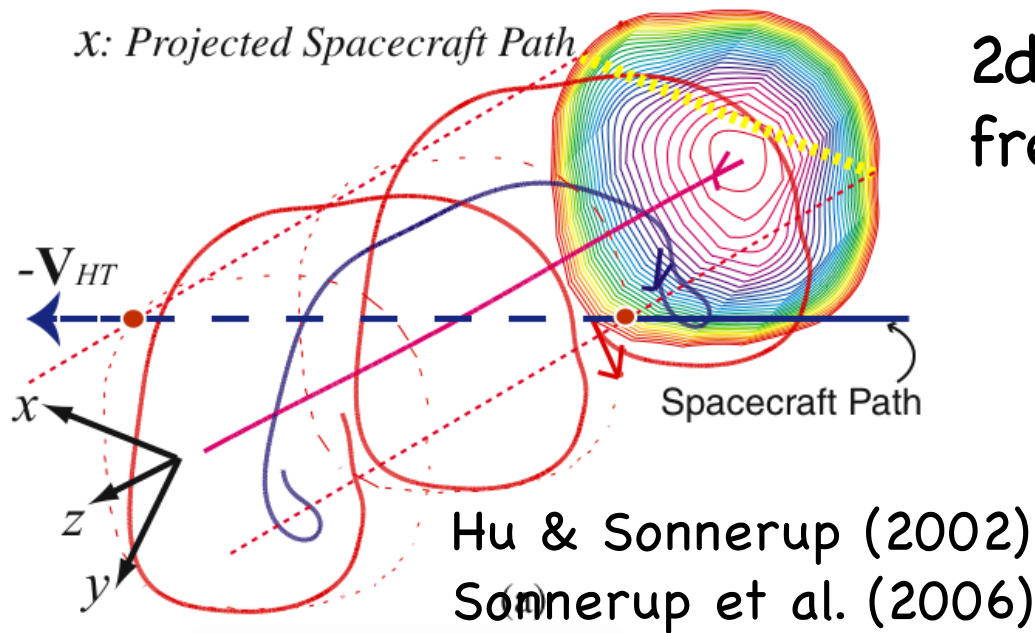
MC flux rope: the Lundquist solution

LEPPING ET AL.: MAGNETIC CLOUDS AT 1 AU



18 MC flux ropes by Lepping et al. 1990,
and 132 MC ropes by Lynch et al. 2005)

MC flux rope: the GS solution



2d magnetostatic non-force-free Grad-Shafranov equation

$$\vec{\nabla} p = \vec{j} \times \vec{B}$$

$$\vec{B} = \left(\frac{\partial A}{\partial y}, -\frac{\partial A}{\partial x}, B_z(A) \right)$$

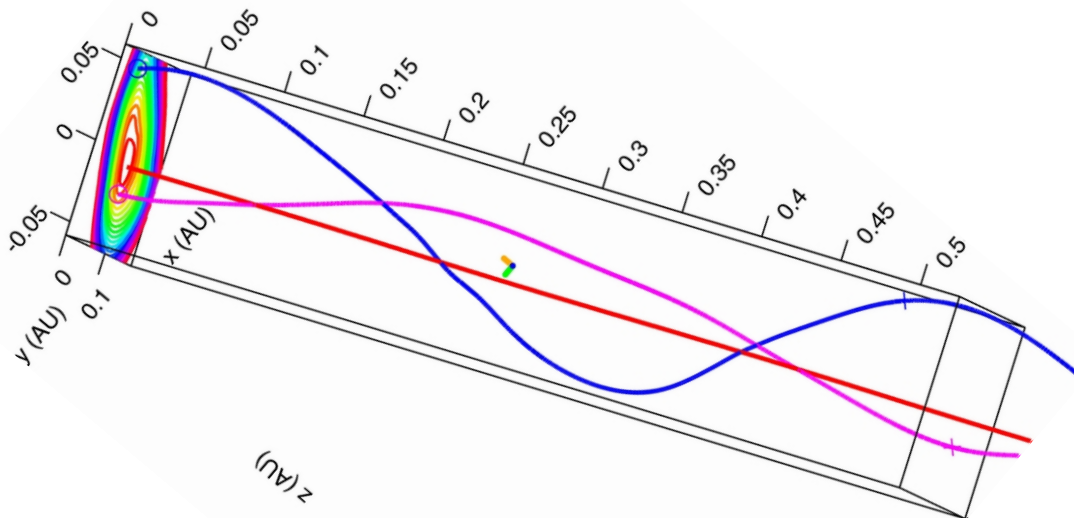
$$P_t(A) = p(A) + B_z^2 / 2\mu_0$$

$$\frac{\partial^2 A}{\partial x^2} + \frac{\partial^2 A}{\partial y^2} = -\mu_0 \frac{dP_t}{dA}$$

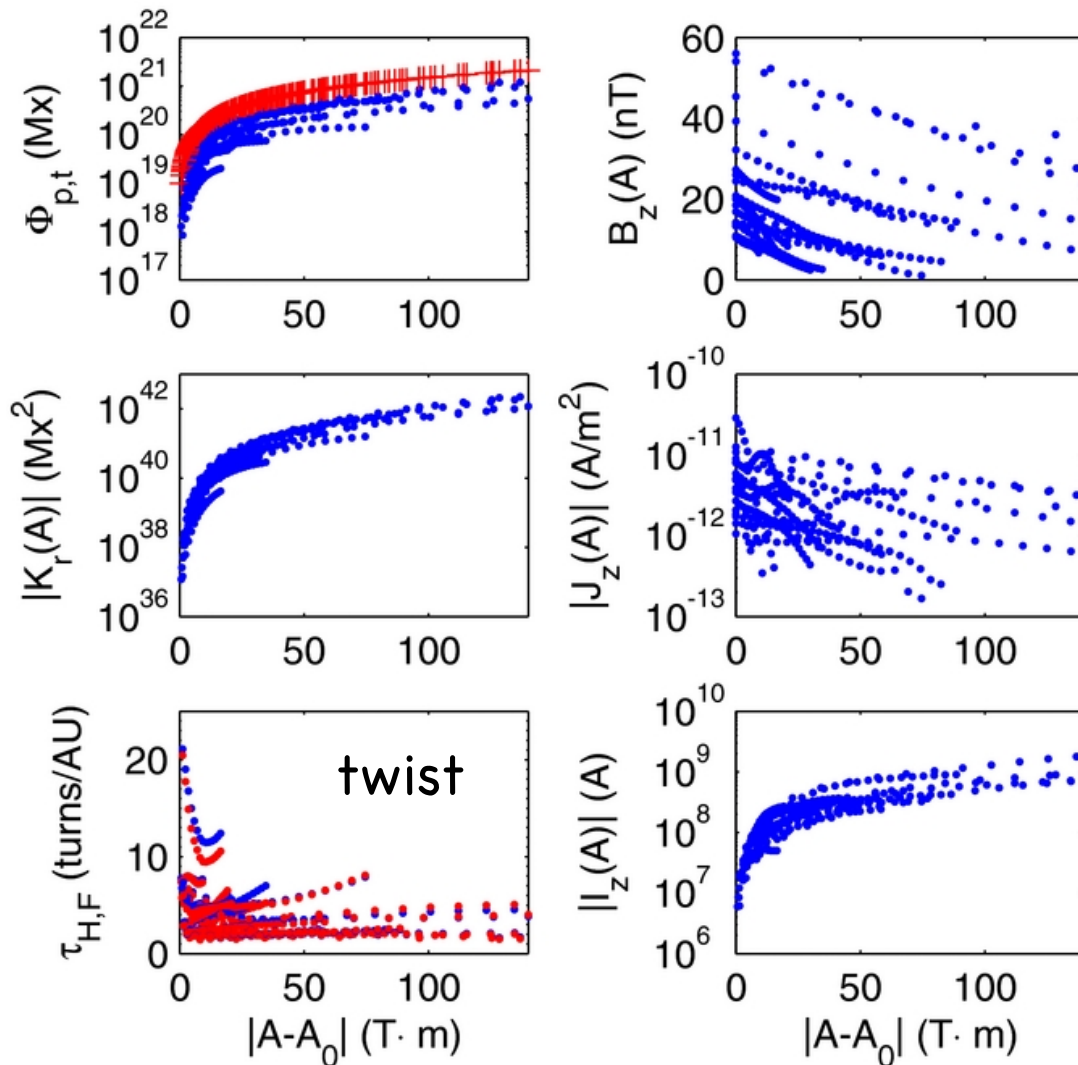
$$\Phi_t = \iint B_z dx dy$$

$$\Phi_p = |A_m - A_b| L$$

$$\tau = 1AU / Lz$$

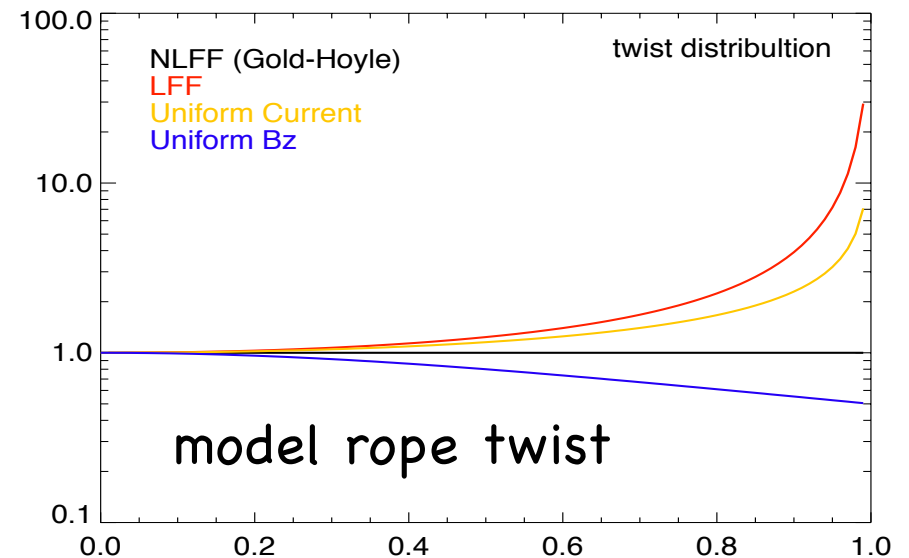


MC flux rope: the GS solution

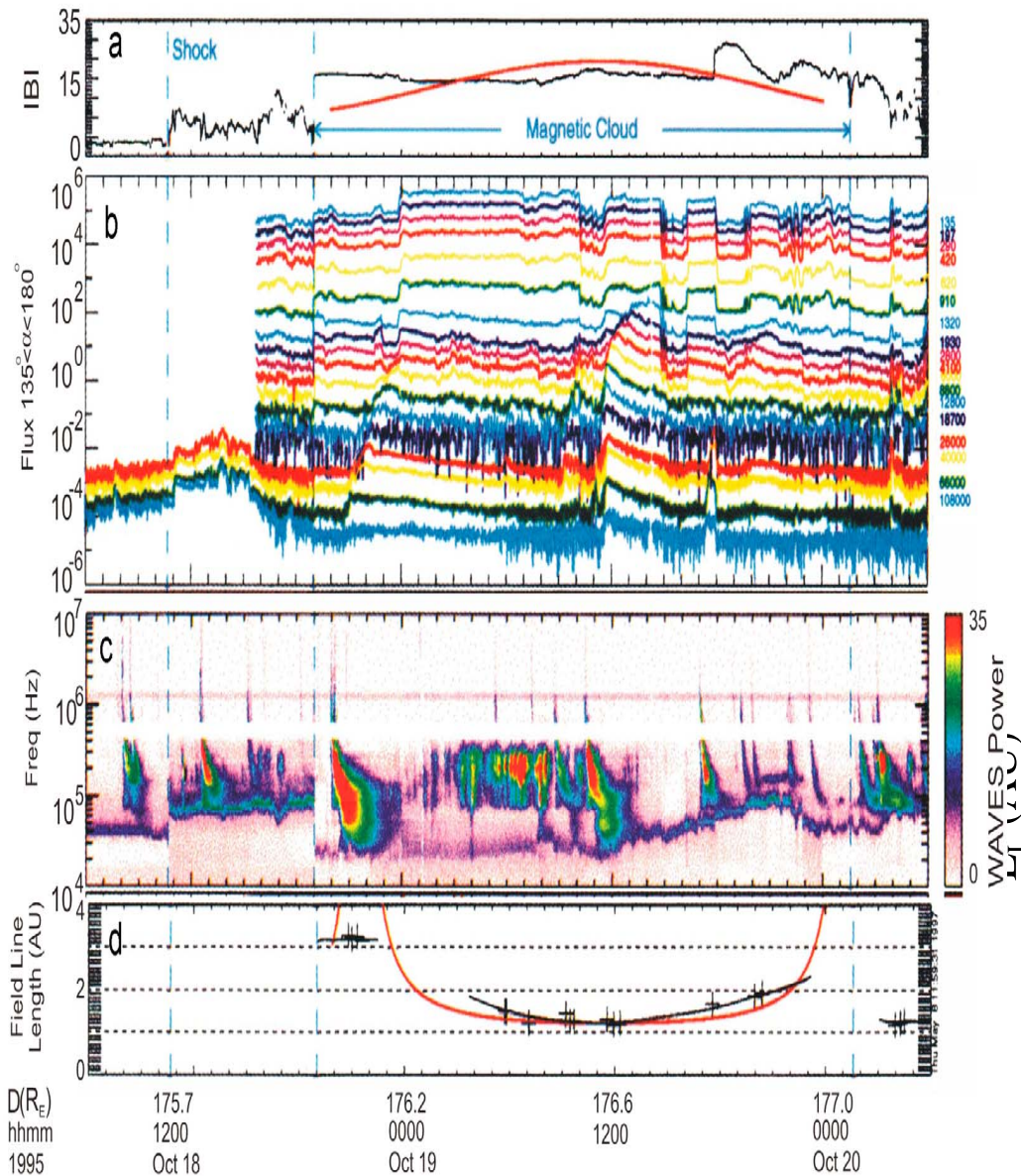


18 MC flux ropes by Hu et al. (2014)

MC flux ropes carry an average twist of $\tau > 3$ per AU. Most of them deviate from the Lundquist solution (Hu et al. 2014, 2015; Kahler et al. 2011).



Field line length of MC flux rope



Lengths of MC field lines are also measured from electron travel times, $L_e = v_e \Delta t$, to compare with models (Larson et al 1997, Kahler et al 2011, Hu et al. 2015)

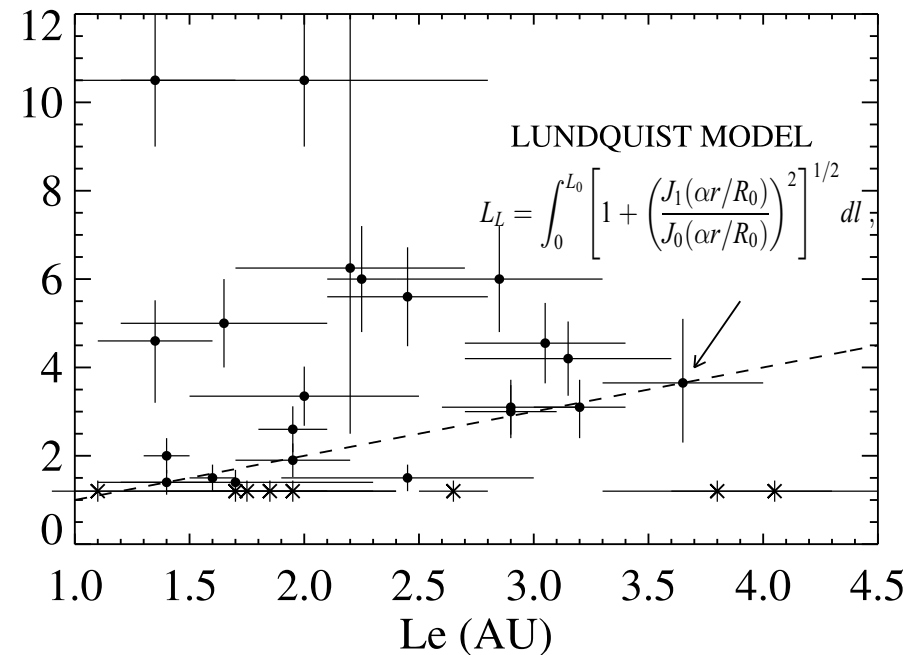


Figure 1 Composite panel of particle and field measurements on the Wind spacecraft in the 19–20 October

properties of MC flux ropes

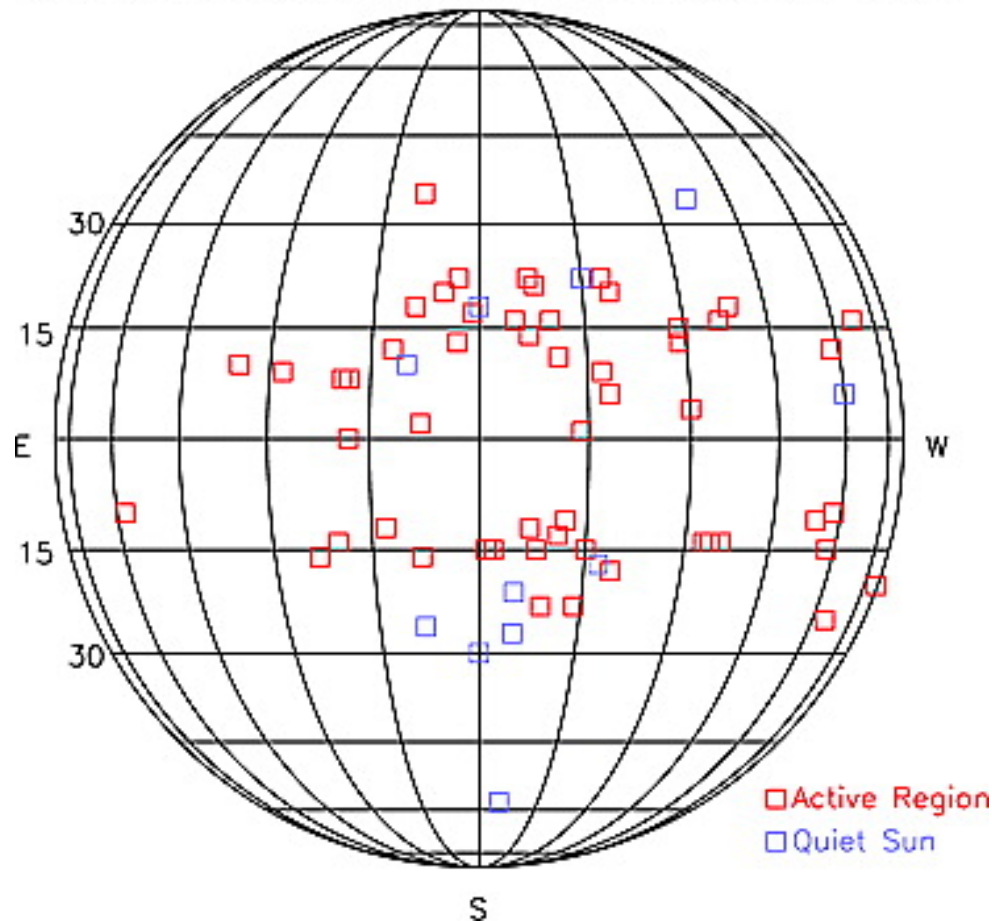
property	typical values at 1 AU
cross-sectional radius (a)	0.1 – 0.5 AU
axial (toroidal) flux	10^{19-21} Mx
azimuthal (poloidal) flux per AU	10^{20-22} Mx
magnetic helicity per AU	10^{40-44} Mx^2
magnetic twist per AU	3 – 5 turns, or more

(Lepping et al. 2000, Lynch et al. 2005, Kahler et al. 2011, Hu et al. 2014)

How are flux ropes formed?

association with solar source regions

Surface Source Regions of Major Geomagnetic Storm



Zhang et al. (2007)

CDAW (1996–2005)
identified solar source
for 88 geomagnetic
storms ($Dst < -100$ nT),
46 being MCs.

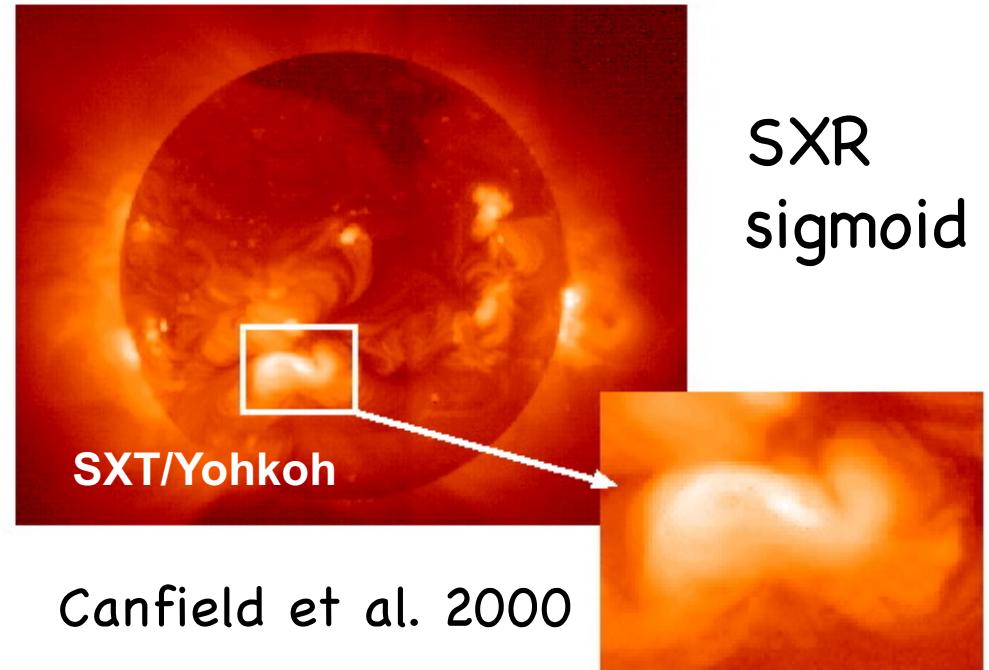
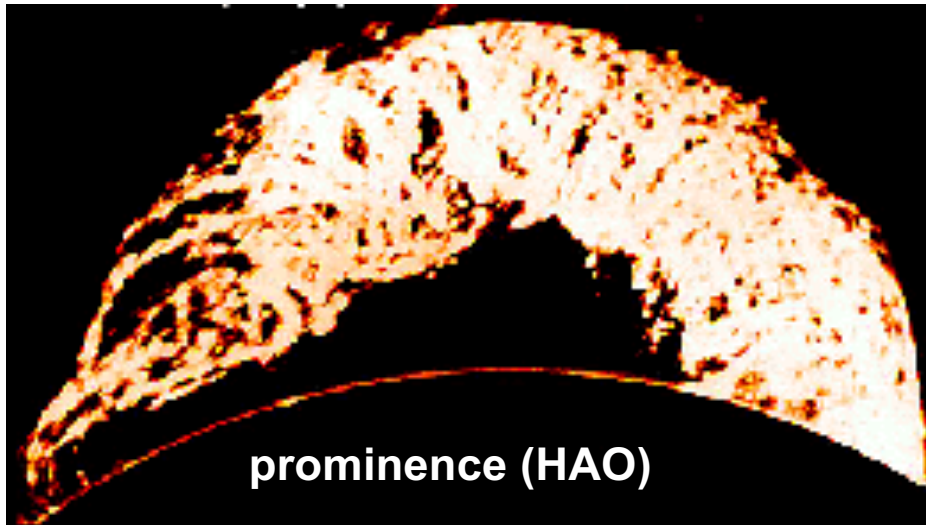
# of MCs (46)	Solar Source
28 (61%)	Active Regions
8 (17%)	Quiet Sun
10 (22%)	unknown

genesis of a flux rope

The debate on nature or nurture: the flux rope is born from below the photosphere (emerging flux rope), or is made in the corona, by reconnection, during its eruption (in-situ formed flux rope), or a hybrid of the two.

	Pre-existing rope	In-situ formed rope
idea	Formed in convection zone, emerges to the corona, or formed in the corona, but prior to eruption	Formed in-situ during eruption by magnetic reconnection
models	Chen89, Low96, Gibson98, Fan04, Forbes-Priest-Isenberg-Lin, VanBallegooijen89	Moore80, Mikic88, Mikic94, Choe96, Demoulin96, Titov99, Antiochos99, Amari03, Longcope07
observations	filaments, sigmoids, other indirect signatures.	sheared arcades, other indirect signatures.
problems	cannot measure magnetic field in the corona	cannot measure magnetic field in the corona

examples of a pre-existing flux rope



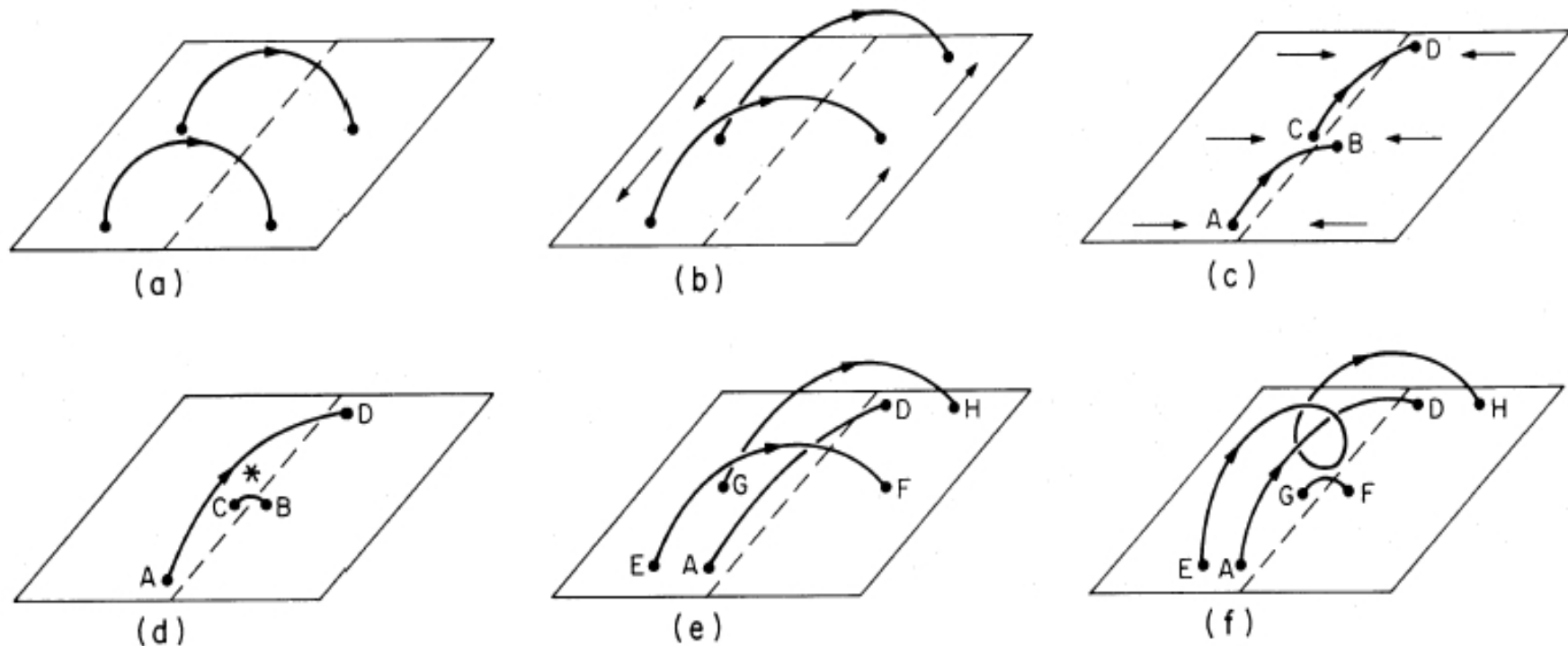
Canfield et al. 2000

Filaments and sigmoids are magnetized plasma structures present prior to eruption with higher chance of MC occurrence.

infer flux rope properties from surface signatures

Physical property	Surface signatures	research
dynamics	CME speed	Gopalswamy01
orientation, handedness	global magnetic field loop arcade filament Sigmoid dimming	Mulligan00 McAllister98 Rust94, Bothmer98 Canfield99, Pevtsov01 Webb00
axial (toroidal) flux	active region filament dimming	Leamon04 Lepping97 Webb00
azimuthal (poloidal) flux, electric current, helicity	active region dimming CME/flare flare	Demoulin02, Nindos03, Leamon04 Mandrini05, Attrill06 Moore07 Longcope07, Qiu07, Kazachenko09,12

flux ropes formed by reconnection



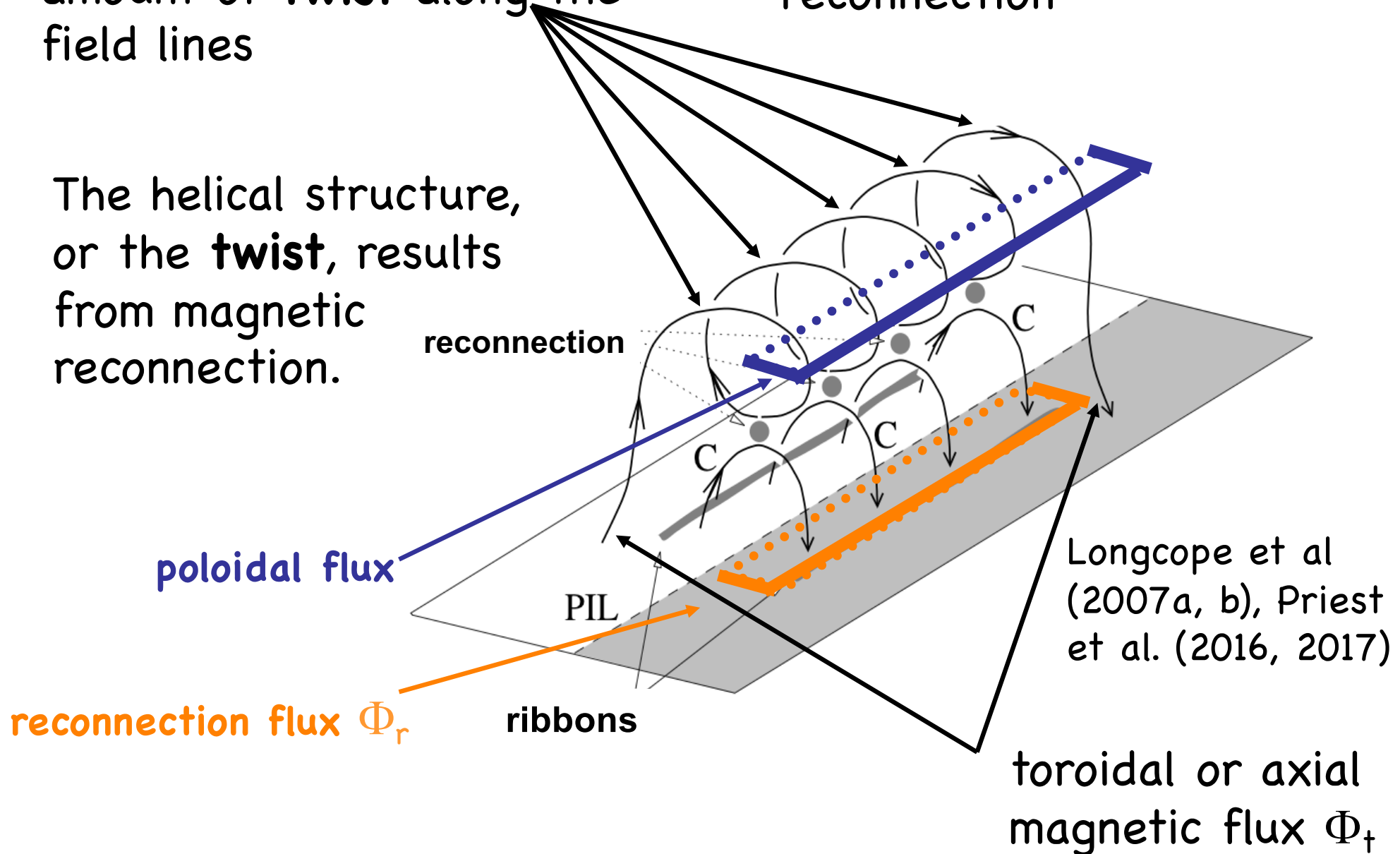
van Ballegooijen & Martens (1989)

Flux rope formed by magnetic reconnection of a sheared arcade, transferring shear to twist.

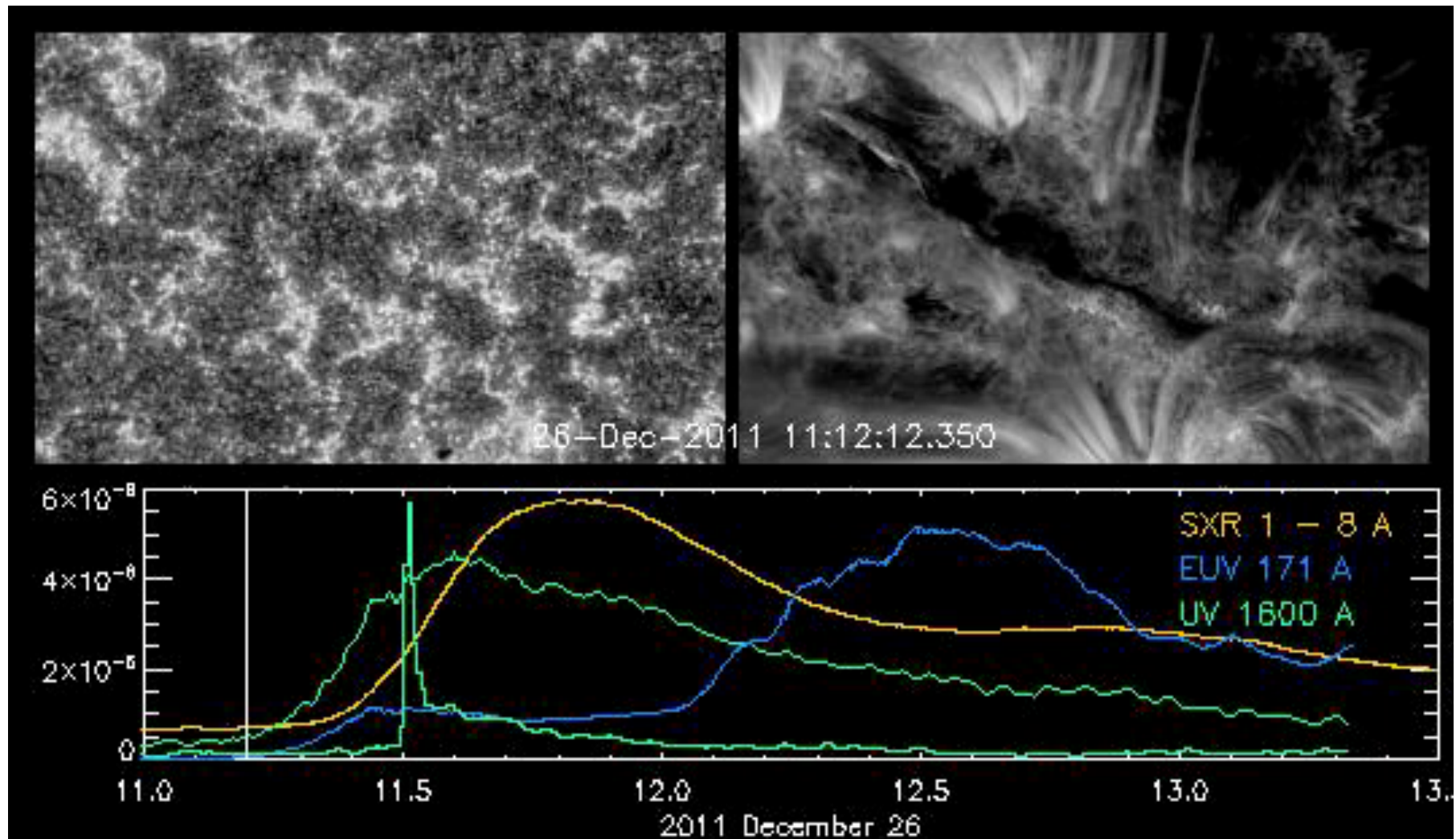
poloidal or azimuthal
magnetic flux Φ_p : the
amount of **twist** along the
field lines

The helical structure,
or the **twist**, results
from magnetic
reconnection.

flux rope formed by
reconnection

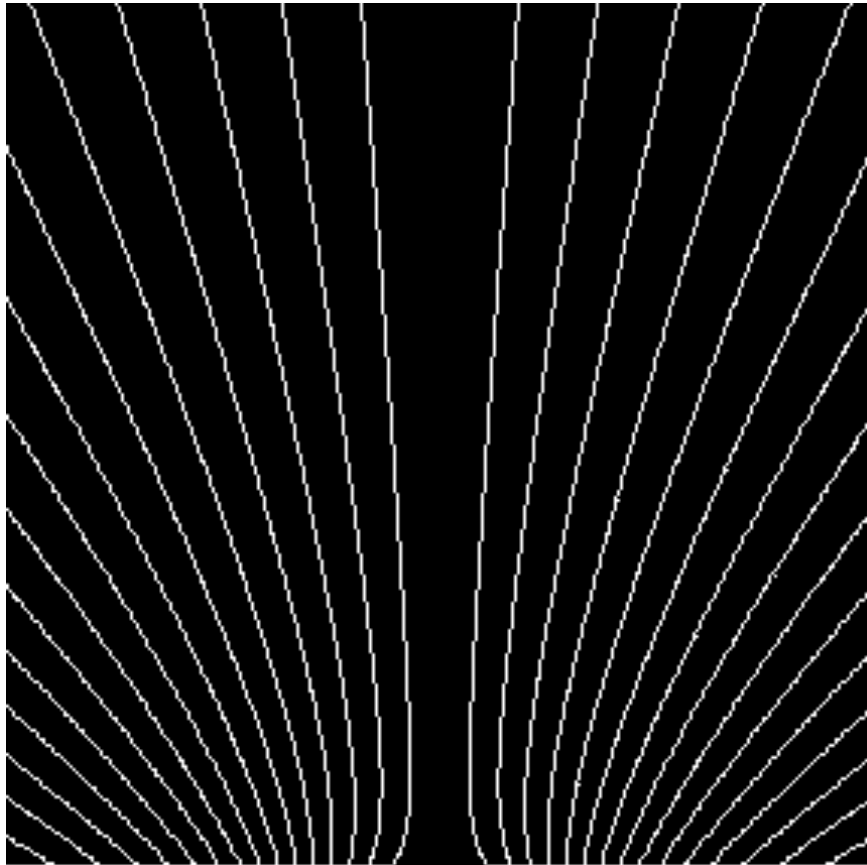


reconnection is “visible” in disk observations

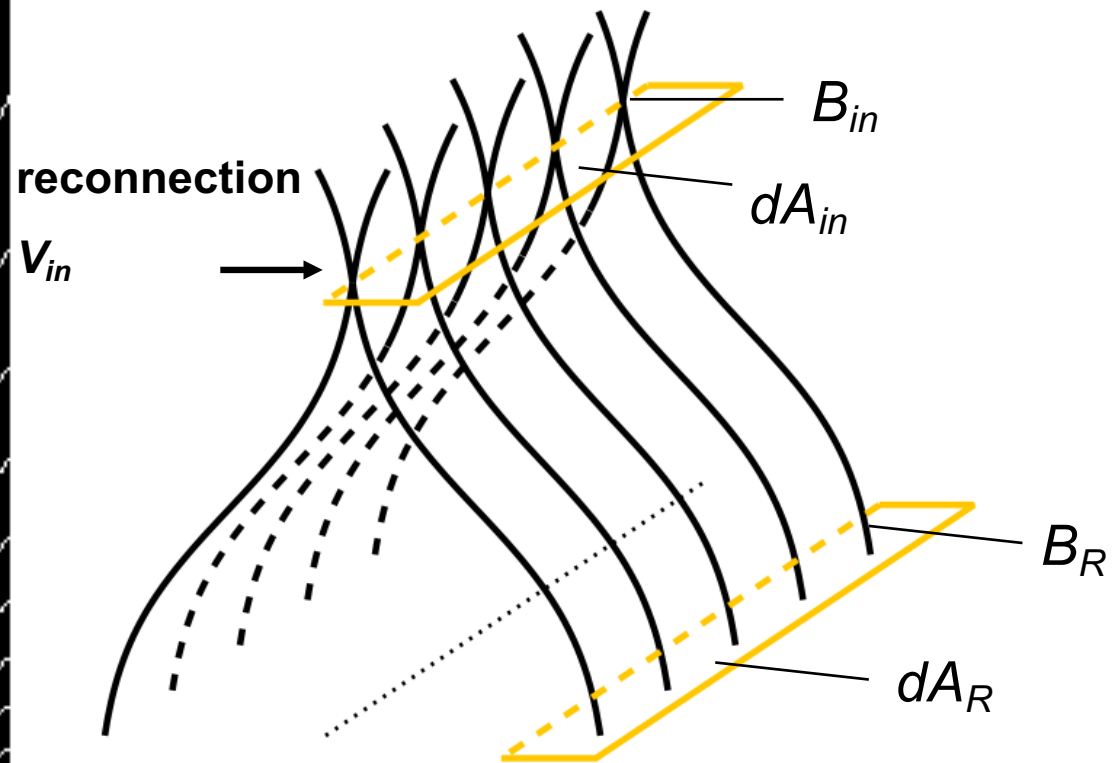


Flare loops and their foot-points are bright because of plasma heating along post-reconnection flux tubes.

reconnection is measured from flare ribbons

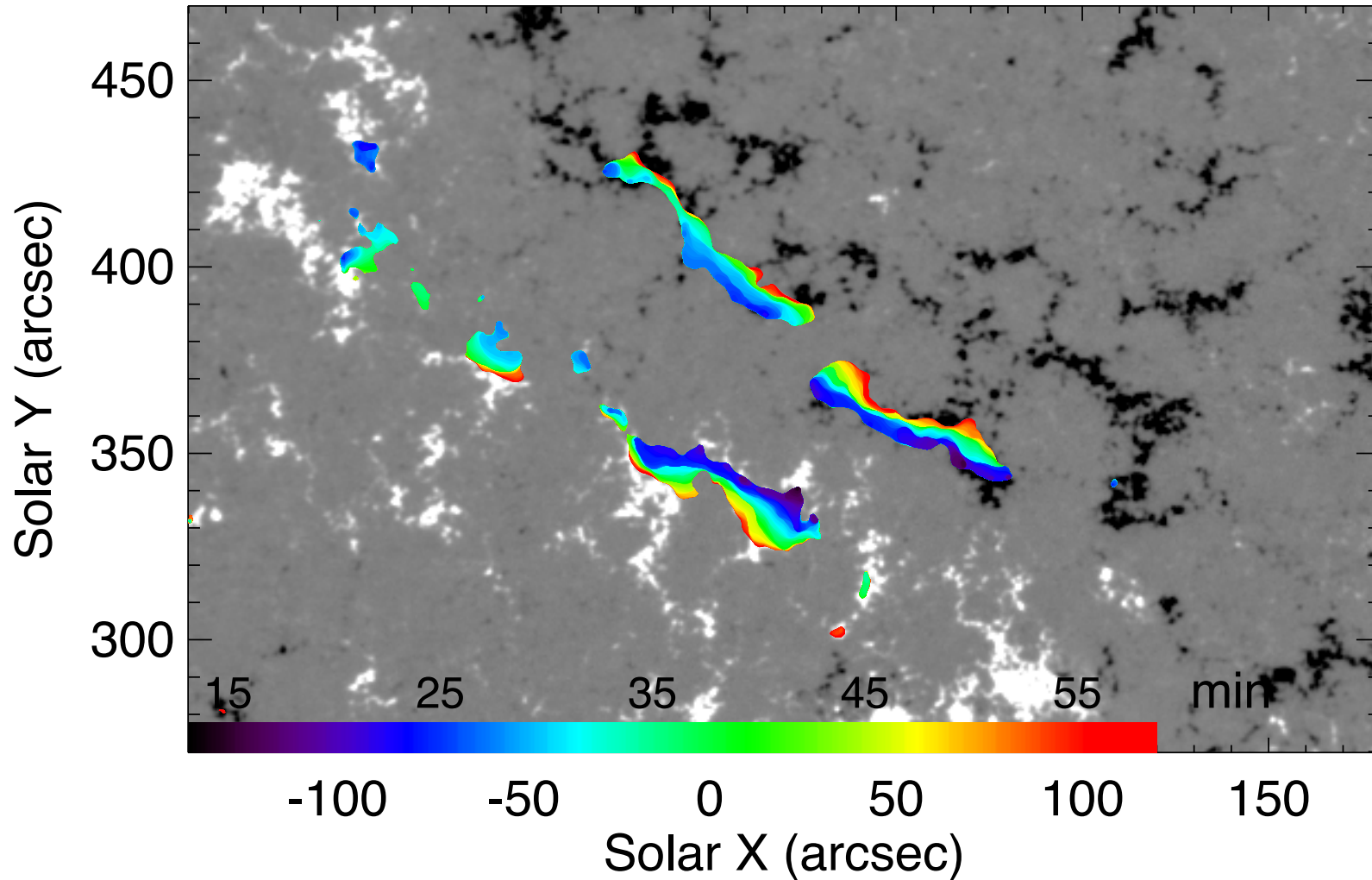


(Terry Forbes)



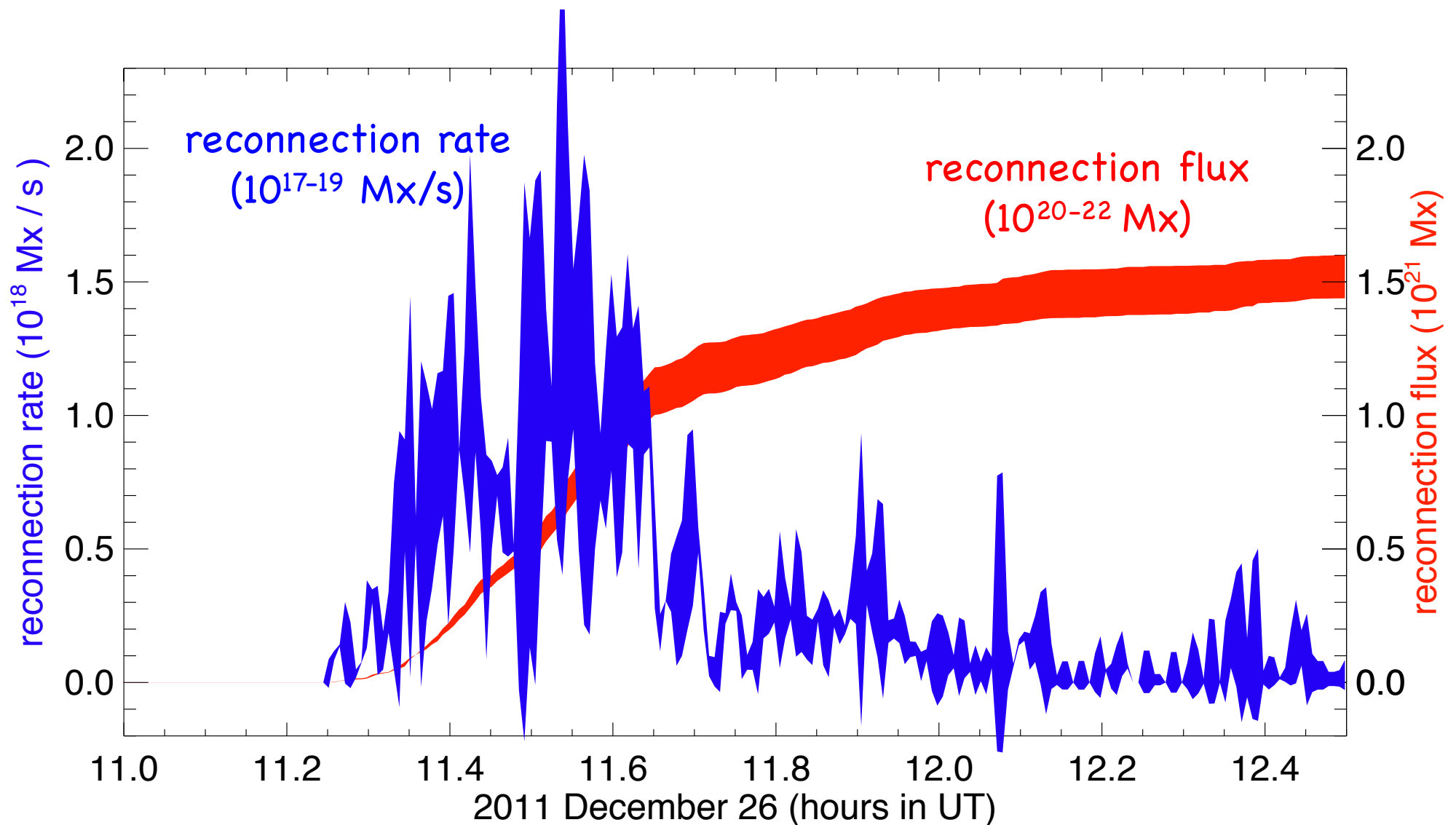
$$\frac{d\Phi_B}{dt} = -\oint \vec{E} \cdot d\vec{l} = \frac{d}{dt} \left(\int B_{in} dA_{in} \right) = \frac{d}{dt} \left(\int B_R dA_R \right) \text{ (Forbes \& Priest 1984)}$$

by mapping ribbons on the magnetogram



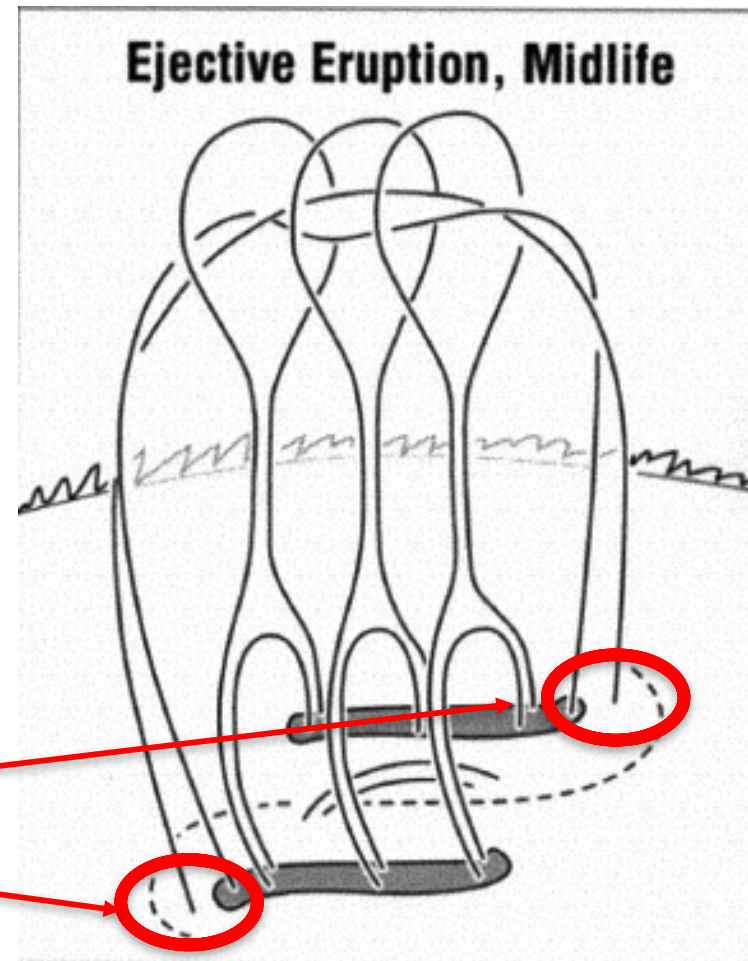
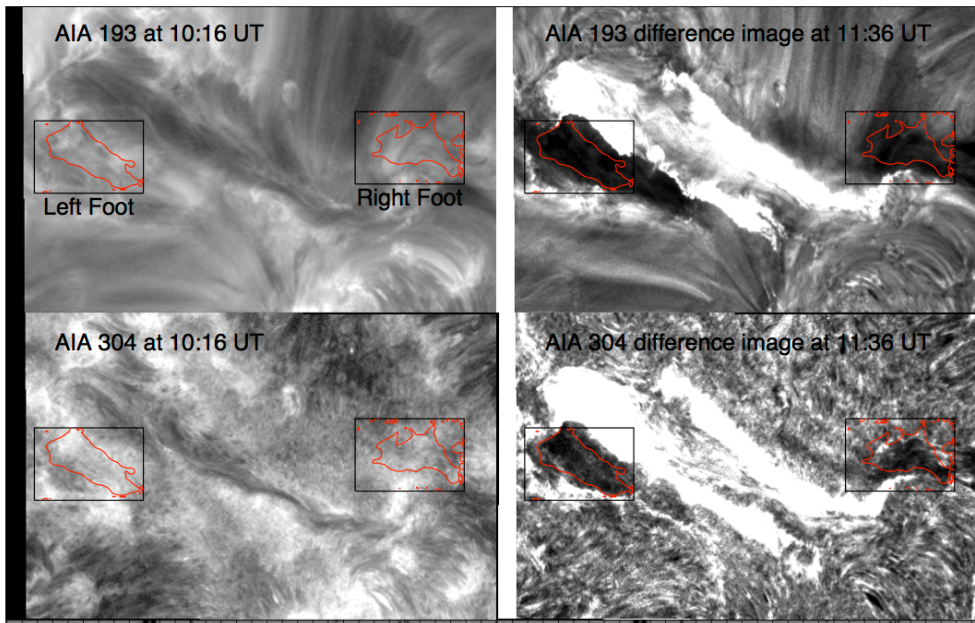
$$\Phi_B = \int B_{in} dA_{in} = \int B_R dA_R$$

reconnection flux is a good fraction of the AR flux



Qiu et al, 2002–2010, Kazachenko et al. (2017)

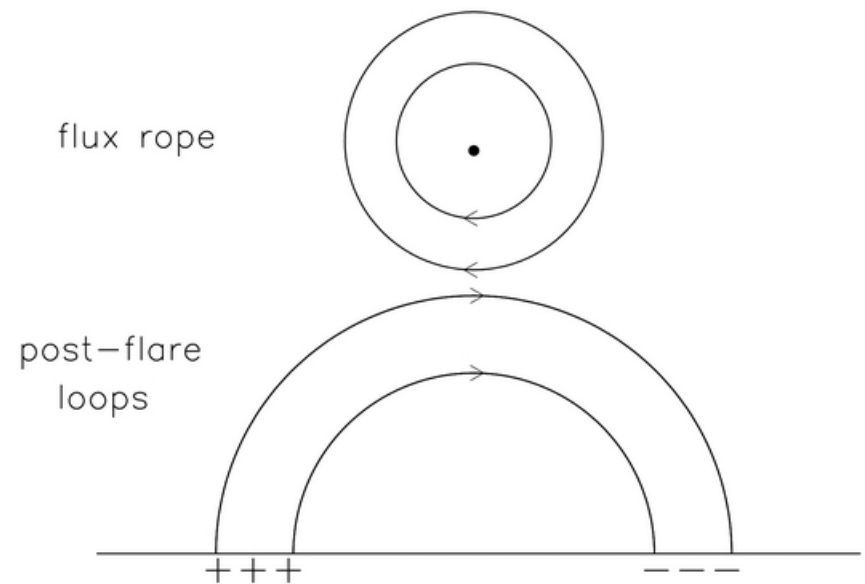
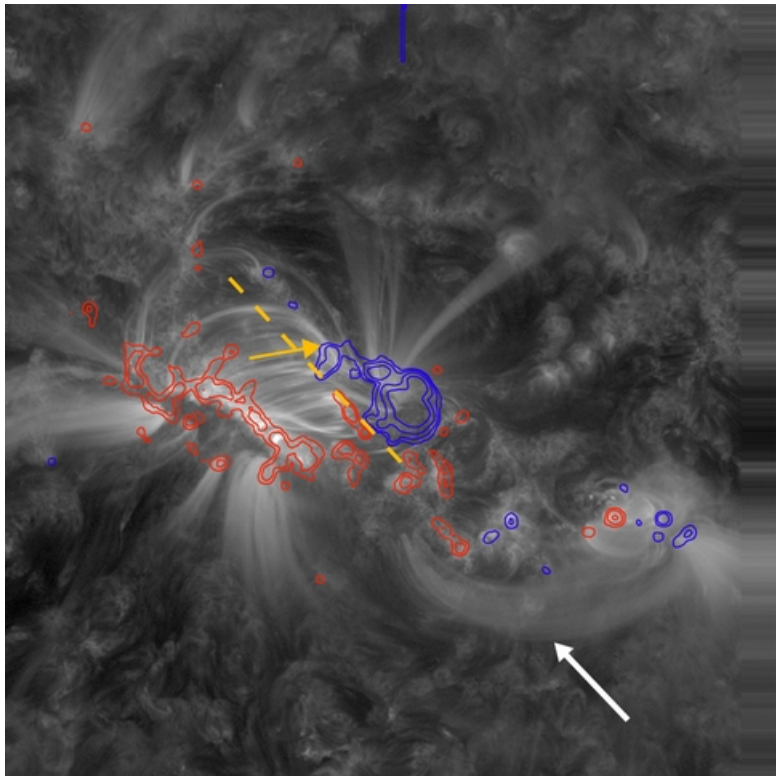
toroidal flux from the standard-model



Moore et al. (2001)

The erupting rope causes **coronal dimming** at the two feet, with which the axial flux of the rope is estimated.

handedness of reconnection formed flux rope



Yurchyshyn et al. 2001, Leamon et al. 2004, Hu et al. 2014

compare MC and solar signatures

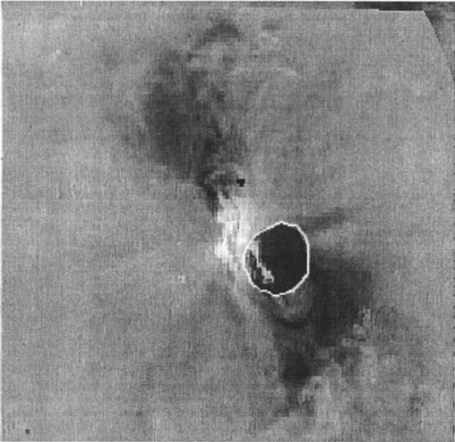
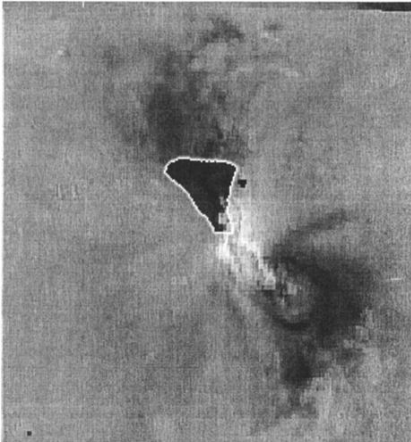
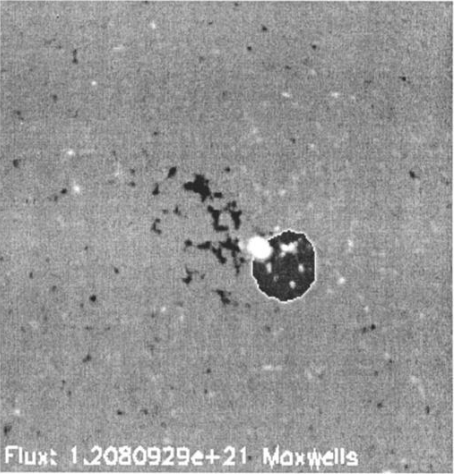
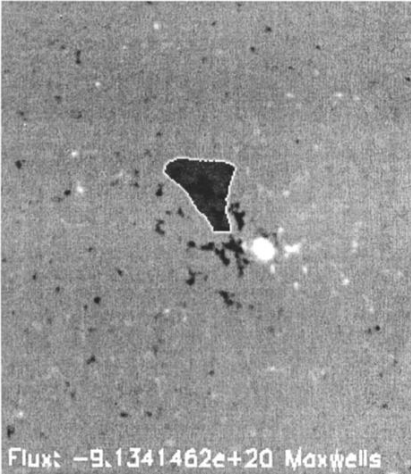
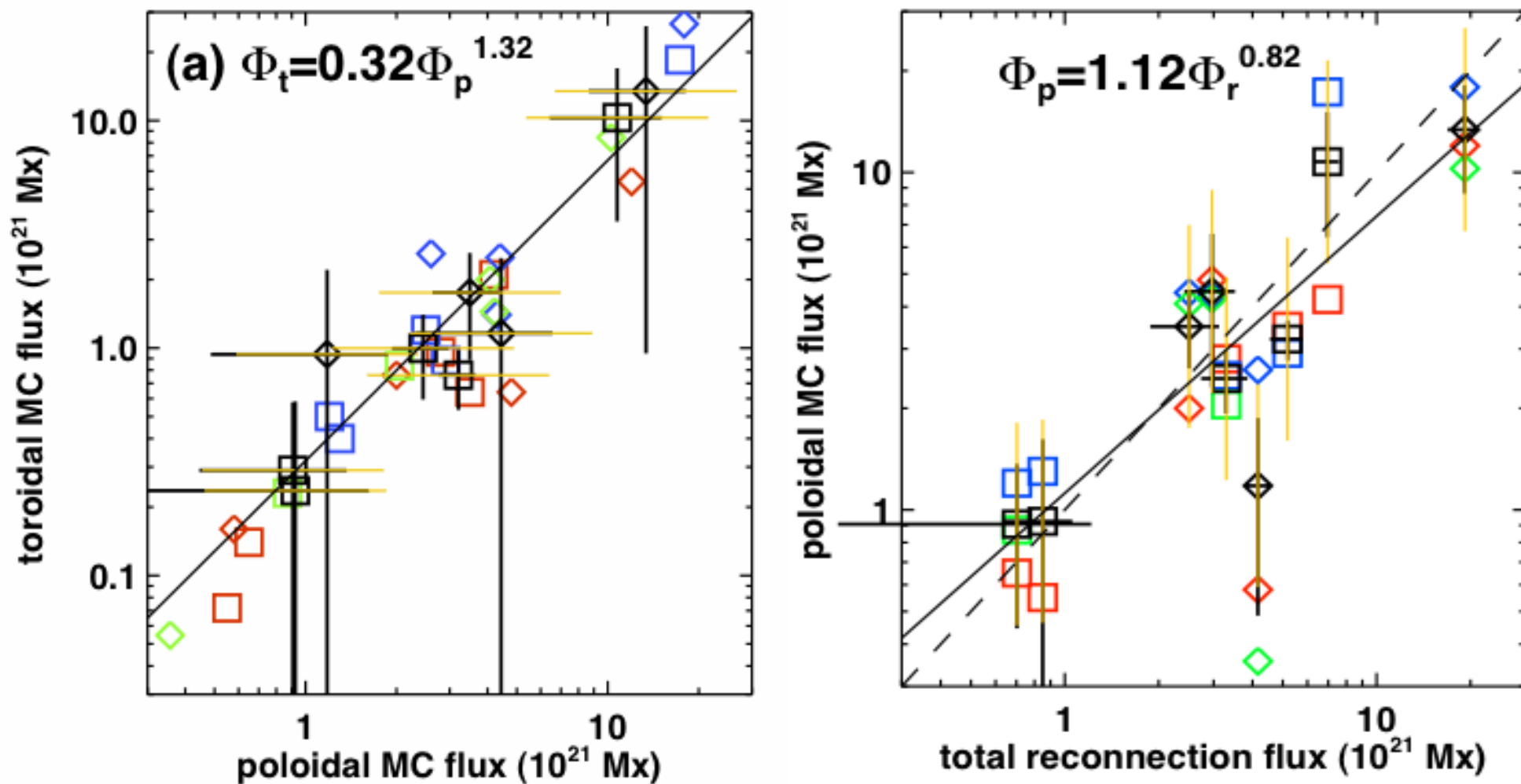
		parameters	Solar surface signatures	MC flux rope
		Projected orientation	45° NE of equator 30° - 55° NE (range) 55° axis of dimmings Filament rotates toward E-W	-11° ecliptic latitude, 108° ecliptic longitude S-E-N type
		handedness	left	left
		Magnetic flux	1.0×10^{21} Mx (dimmings)	7.35×10^{20} Mx (axial)
		speed	600 km/s (CME front)	430-500 km/s

Figure 3. (Top) EIT difference image (0507 UT-0450 UT) and (bottom) MDI image (0454 UT). Superposed are the area masks which were used to estimate total magnetic flux at the assumed footpoints of erupting loop system. Masks used for the southwest (left) and northeast (right) dimming regions.

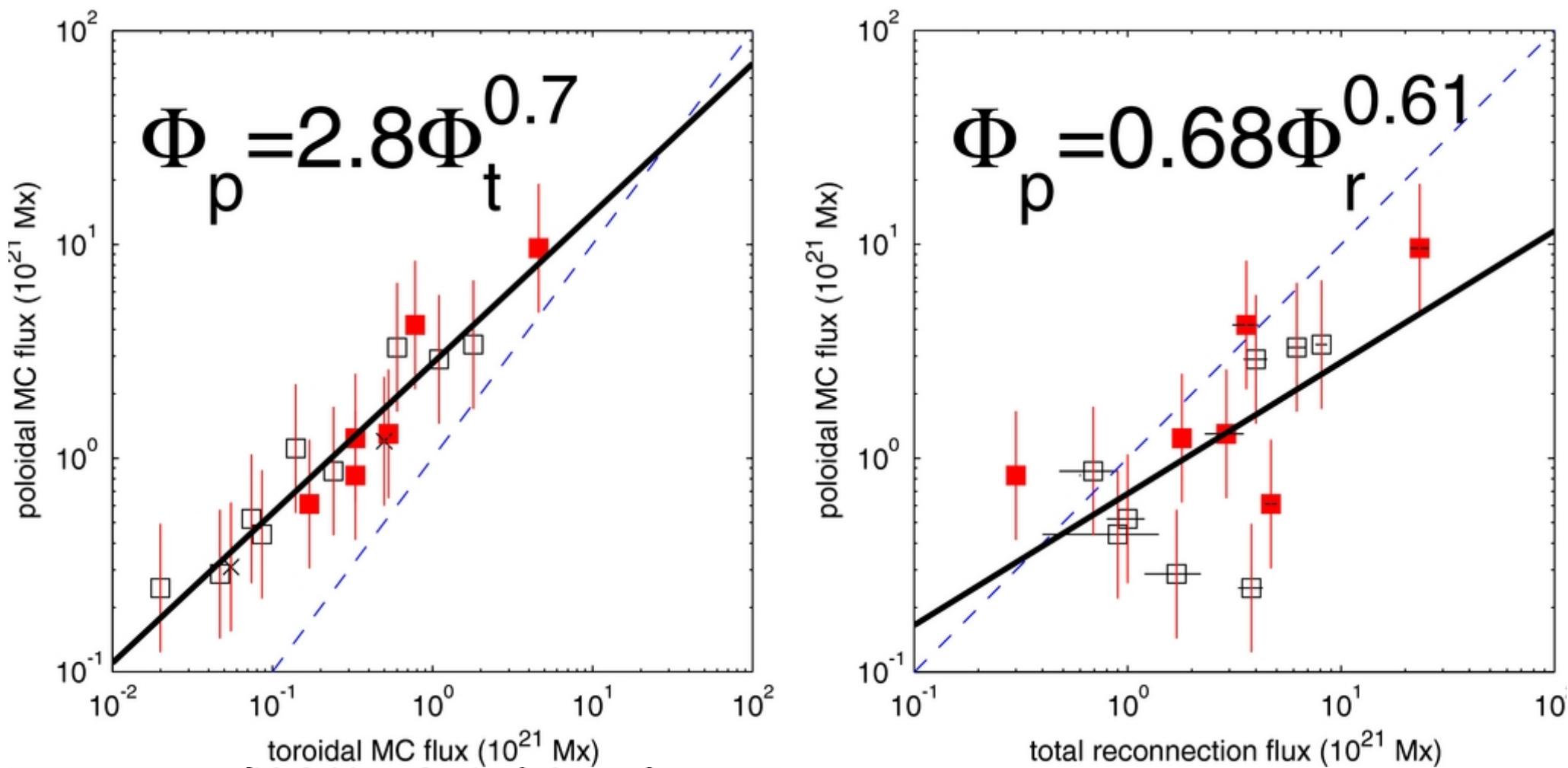
An event on 1997 May 12-15 analyzed by Webb et al. (2000)

reconnection flux and MC flux



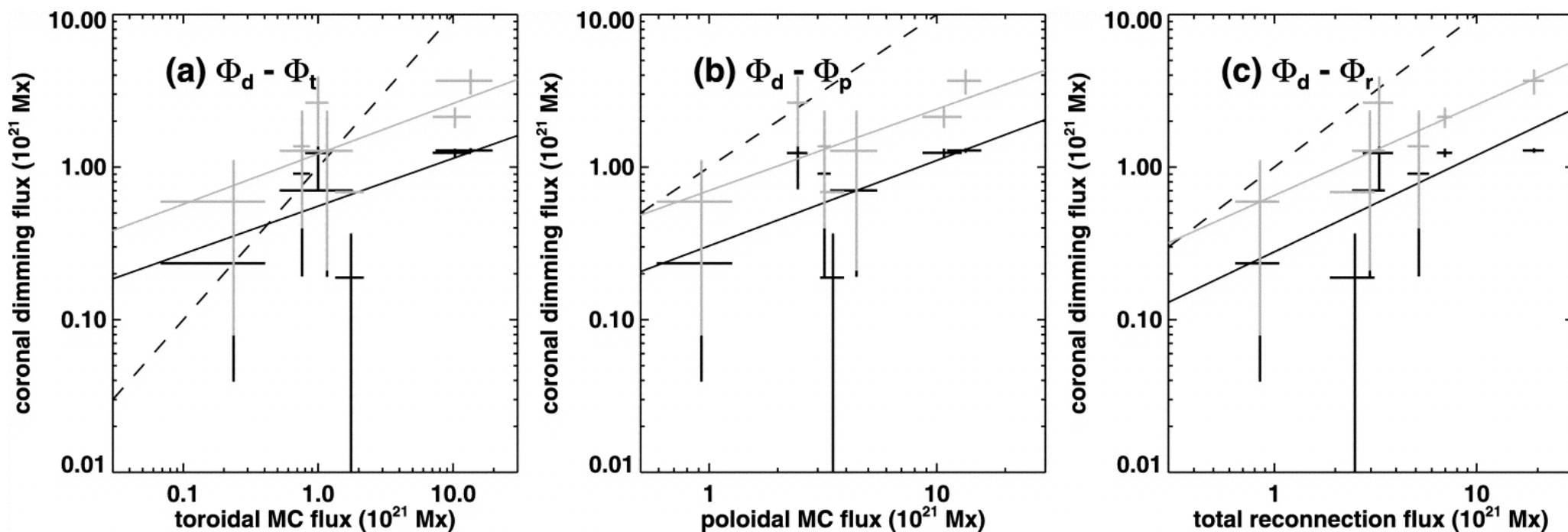
(Qiu et al. 2007, Hu et al. 2014)

reconnection flux and MC flux



(Qiu et al. 2007, Hu et al. 2014)

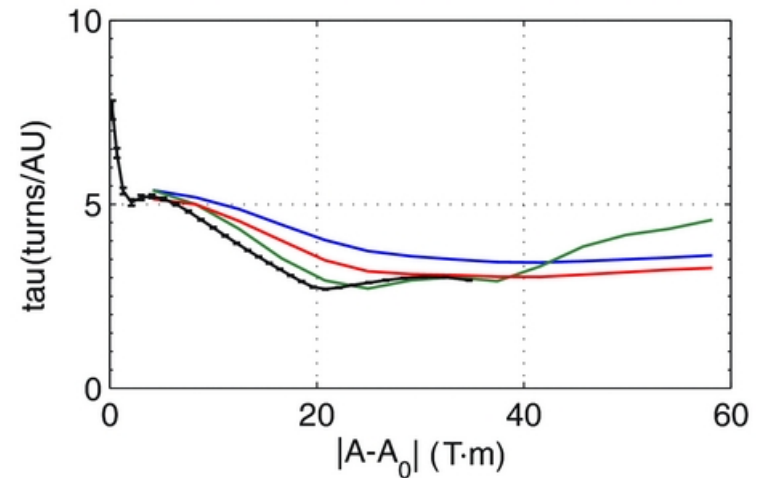
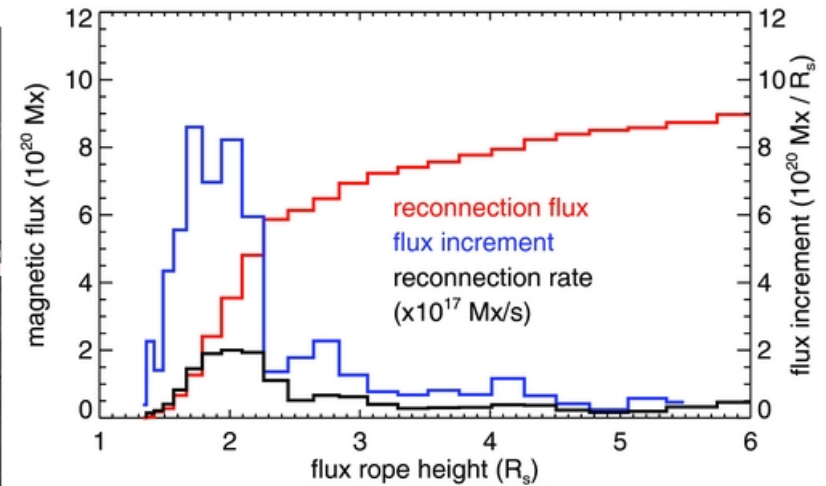
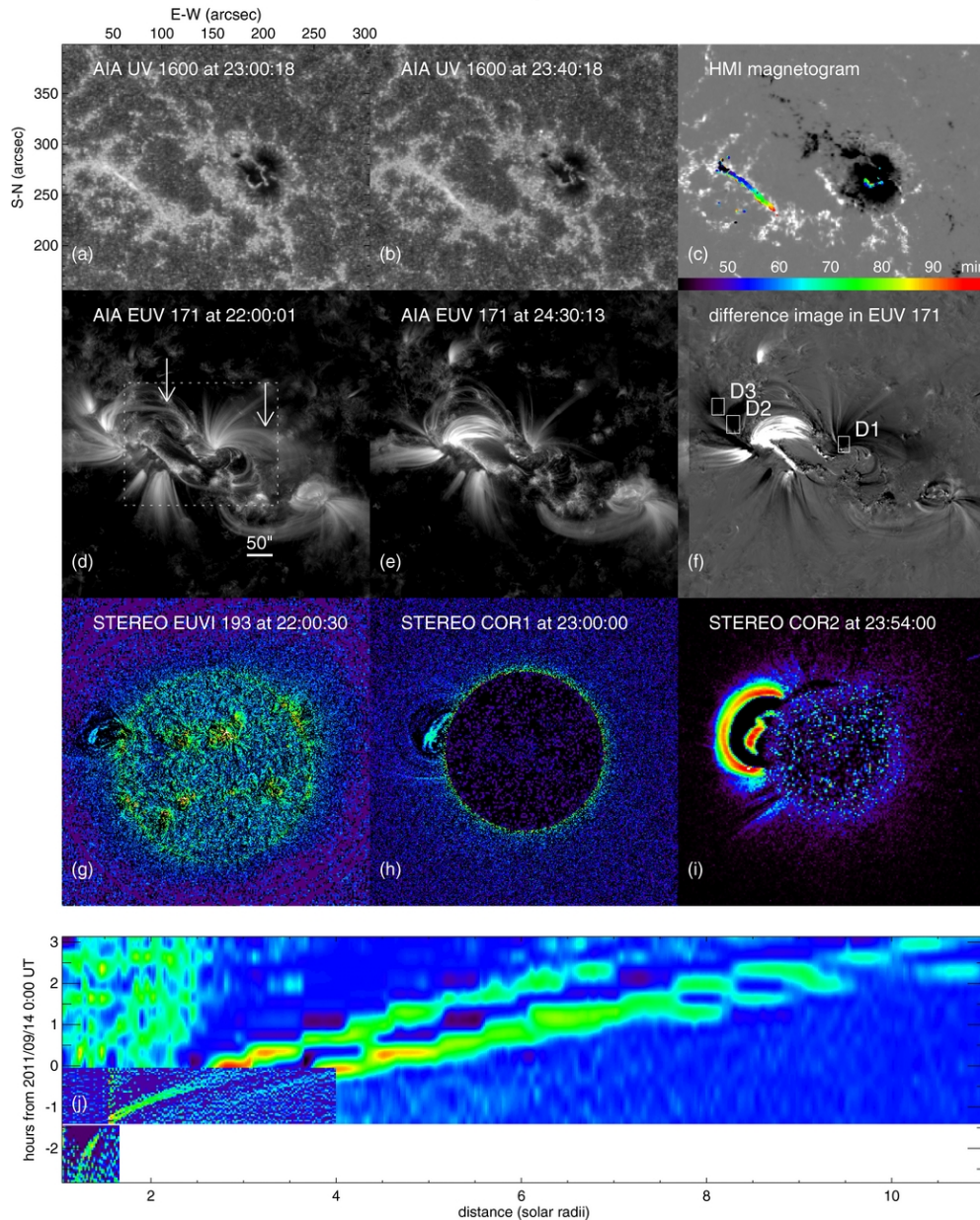
dimming flux and MC flux



(Qiu et al. 2007, Mandrini et al. 2005, Attrill et al. 2006)

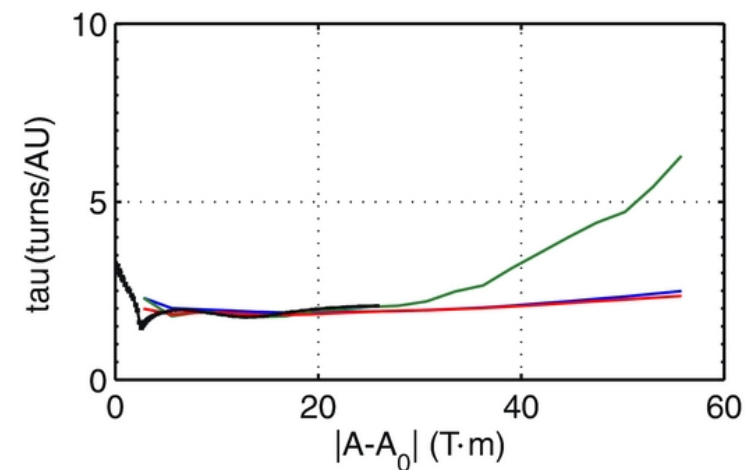
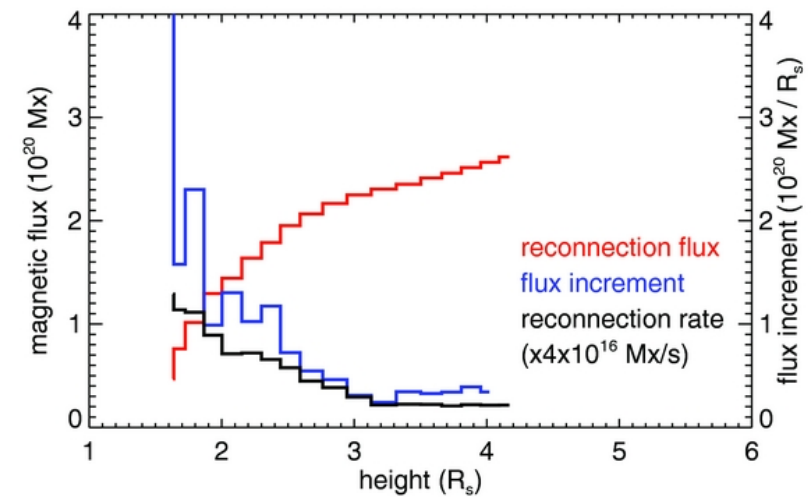
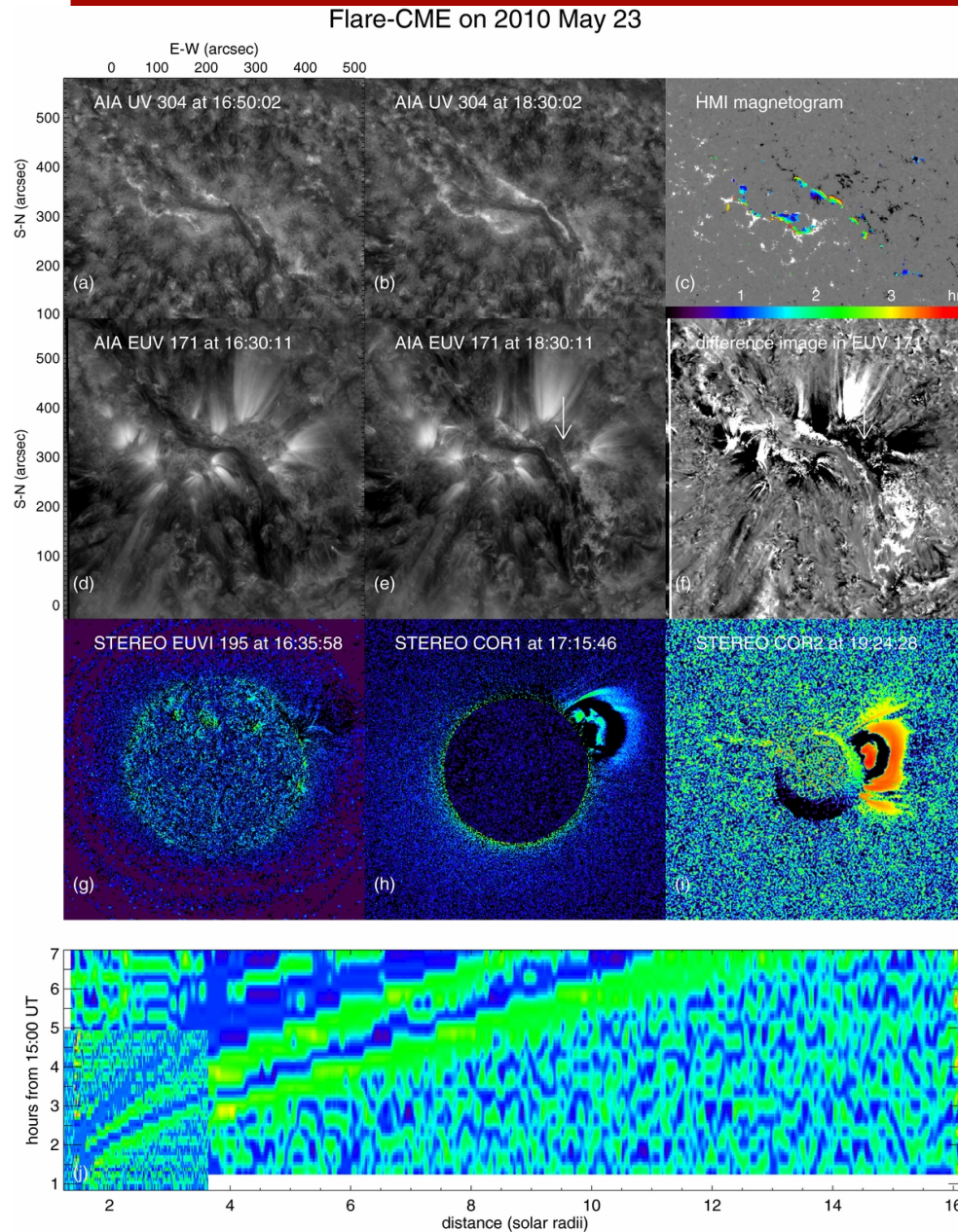
flare configuration and MC twist

Flare-CME on 2011 September 13 - 14



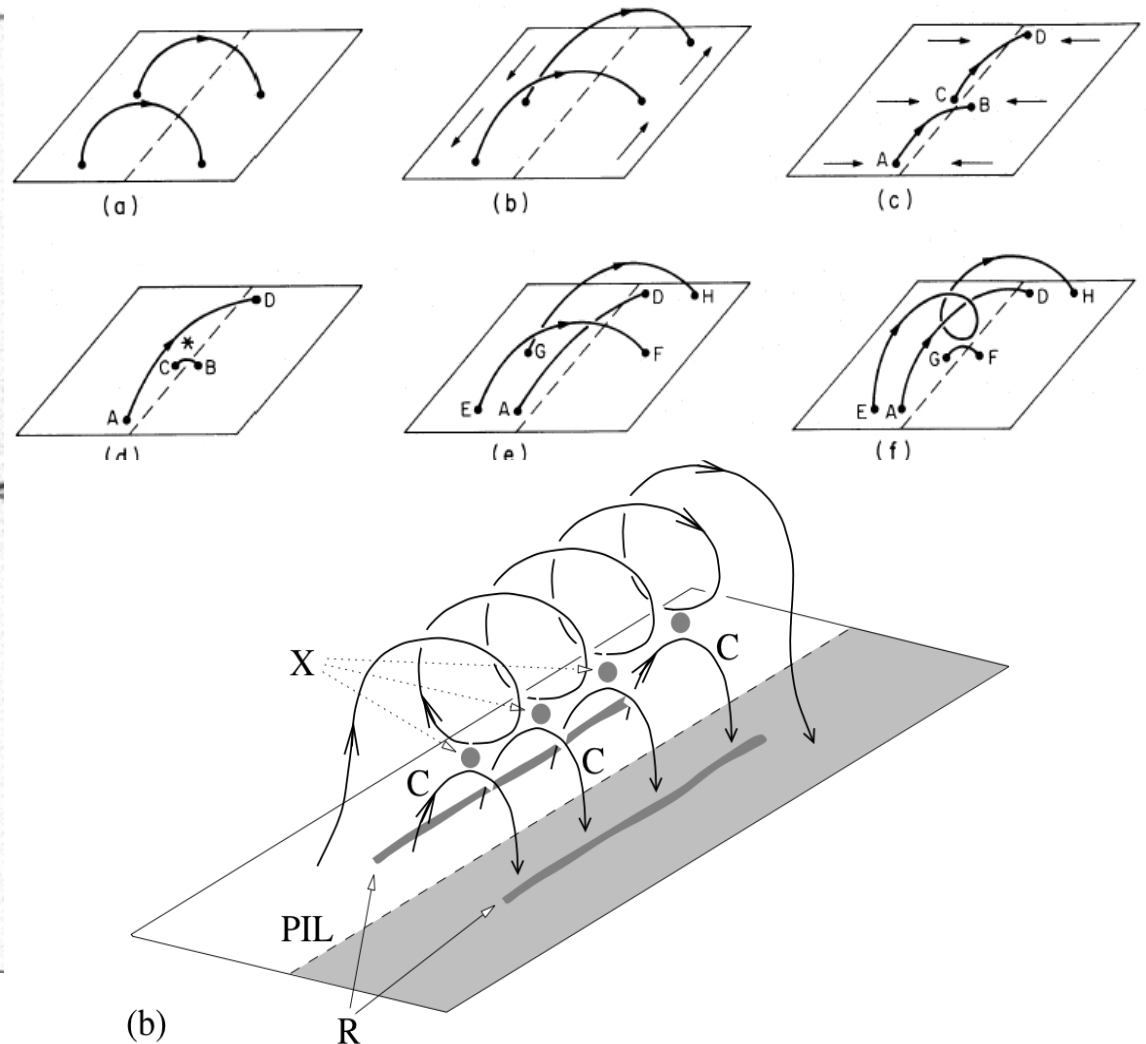
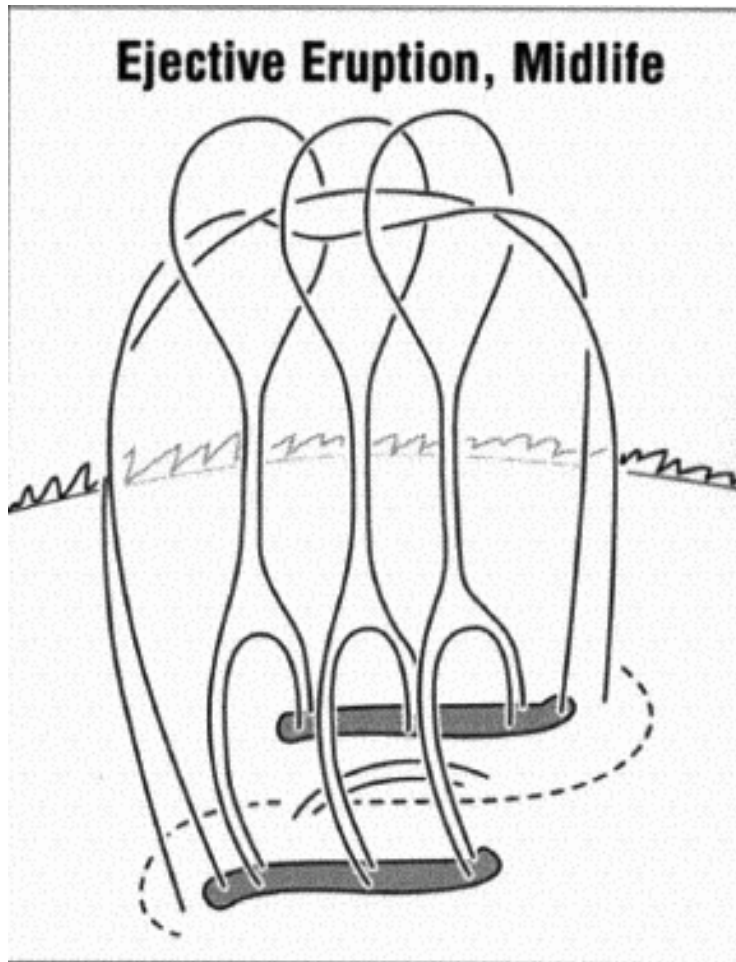
An event with decreasing twist (Hu et al. 2014)

flare configuration and MC twist



An event with flat twist (Hu et al. 2014)

flare configuration and MC twist



Which one is correct? What do we see in MC flux rope and flare? (Priest et al. 2016, 2017)

Summary

MC measurements provide evidence of flux ropes, which probably carry a large amount of twist.

MC flux ropes are formed in the Sun, and reconnection plays an important role in its formation, as well as its energetics.